

Scaling symmetry, renormalization, and time series modeling

Marco Zamparo*

HuGeF, Via Nizza 52, 10126 Torino, Italy

Fulvio Baldovin,[†] Michele Caraglio,[‡] and Attilio L. Stella[§]

*Dipartimento di Fisica e Astronomia, Sezione INFN, CNISM,
Università di Padova, Via Marzolo 8, I-35131 Padova, Italy*

(Dated: June 7, 2018)

We present and discuss a stochastic model of financial assets dynamics based on the idea of an inverse renormalization group strategy. With this strategy we construct the multivariate distributions of elementary returns based on the scaling with time of the probability density of their aggregates. In its simplest version the model is the product of an endogenous auto-regressive component and a random rescaling factor designed to embody also exogenous influences. Mathematical properties like increments' stationarity and ergodicity can be proven. Thanks to the relatively low number of parameters, model calibration can be conveniently based on a method of moments, as exemplified in the case of historical data of the S&P500 index. The calibrated model accounts very well for many stylized facts, like volatility clustering, power law decay of the volatility autocorrelation function, and multiscaling with time of the aggregated return distribution. In agreement with empirical evidence in finance, the dynamics is not invariant under time reversal and, with suitable generalizations, skewness of the return distribution and leverage effects can be included. The analytical tractability of the model opens interesting perspectives for applications, for instance in terms of obtaining closed formulas for derivative pricing. Further important features are: The possibility of making contact, in certain limits, with auto-regressive models widely used in finance; The possibility of partially resolving the long-memory and short-memory components of the volatility, with consistent results when applied to historical series.

I. INTRODUCTION

Time series analysis plays a central role in many disciplines, like physics [1], seismology [2], biology [3], physiology [4], linguistics [5], or economy [6], whenever datasets amount to sequences of measurements or observations. A main goal of such analysis is that of capturing essential regularities of apparently unpredictable signals within a synthetic model, which can be used to get forecasts and a deeper understanding of the mechanisms governing the processes under study. A satisfactory time series modeling for complex systems may become a challenging task, due to the need to account for statistical features of the data connected with the presence of strong correlations. In the last decades, features of this kind have been extensively studied in the context of financial time series, where they strongly stimulated the search for adequate stochastic modeling [3, 7, 9]. The non-Gaussianity of the probability density function (PDF) of aggregated returns of an asset over time intervals in substantial ranges of scales, its anomalous scaling and multiscaling with the interval duration, the long-range dependence of absolute return fluctuations (volatility), the violation of time-reversal symmetry, among other robust statistical features called *stylized facts* in finance [10, 11],

still remain elusive of synthetic and analytically tractable modeling. Besides the standard model of finance based on geometric Brownian motion [7, 12], proposed descriptions include stochastic volatility models (See, e.g., [9] and references therein), multifractal models inspired by turbulence [13–18], multi-timescale models [19, 20], various types of self-similar processes [21–26], multi-agent models [27–29], and those in the Auto-Regressive Conditional Heteroskedastic (ARCH) and Generalized-ARCH (GARCH) family [3, 30–32].

To be effective, a stochastic model should not only correctly reproduce the statistical features observed in the empirical analysis, but also be easy to calibrate and analytically tractable in order to be useful in applications like derivative pricing and risk evaluation [7, 33]. In this respect, research in stochastic modeling of financial assets is still a challenging topic [18]. Recently, some of us proposed an approach to market dynamics modeling [23, 34] inspired by the renormalization group theory of critical phenomena [43–45]. The background ideas exposed in Refs. [23, 34] already stimulated some contributions along various lines [23–26, 35–37]. In particular, in [25] a model with nonstationary increments and lacking a volatility feedback mechanism has been discussed in detail, pointing out its potential interest and missing features. In the present Paper, we make a step forward along the lines proposed in [23], by introducing a novel discrete-time stochastic process characterized by both an auto-regressive endogenous component and a short-memory one. The first provides a volatility feedback thanks to its long dynamical memory; the latter represents, besides immediate endogenous mechanisms, also the impact of

*Electronic address: marco.zamparo@hugef-torino.org

†Electronic address: baldovin@pd.infn.it

‡Electronic address: caraglio@pd.infn.it

§Electronic address: stella@pd.infn.it

external influences. Many features of the model are under analytical control and a number of basic properties, like increments' stationarity, time-reversal asymmetry, strong mixing and ergodicity as a consequence, can be proved. In addition, an explicit procedure for calibrating its few parameters makes the model a candidate for applications, e.g., to derivative pricing [7, 33], for which useful closed expressions can be derived [38]. An interesting feature of our approach is the possibility of resolving the long-memory and short-memory components of the volatility. This could be exploited in order to partially separate exogenous and endogenous mechanisms within the market dynamics. The version of the model we discuss within the present Paper does not include skewness in the return PDF and the leverage effect [7, 39]. However, here we outline simple ways of improving it in order to consistently recover also these effects.

While some analytical derivations and detailed proofs are reported in the Supplementary Material [40], in the main text we illustrate the general ideas inspiring the model, we discuss its properties, and show that they allow to implement a successful calibration protocol. Specifically, we use the model to reproduce the daily historical time series of the S&P500 index in the years 1950-2010. The Paper is organized as follows. The next Section contains a description of the background ideas inspiring the model construction, whose precise definition is reported in Section III. This Section also describes a simple parametrization in which contact with a Markov-switching ARCH process (SWARCH) is realized. Section IV is then devoted to a brief review of the properties of the model. Section V proposes a simple calibration scheme, whereas a comparison with historical series is discussed in Section VI. Section VII deals with the interesting question about identifying the long-memory and short-memory components in empirical time series. In Section VIII we discuss the possibility of describing skewness and the leverage effect and mention other perspective developments. Finally, in Section IX we draw our conclusions.

II. SCALING AS A GUIDING SYMMETRY

Since the pioneering work of Mandelbrot and van Ness on fractional Brownian motion [41], interest in scaling features has characterized many models of financial and other time series, especially in contributions by members of the physics community. Proposals include the representation of financial processes as truncated Levy flights [21, 22], or the more sophisticated descriptions through multifractal cascades inspired by turbulence [13–18]. In the financial literature, a similar focus on scaling properties is harder to find. Indeed, although leptokurtic distributions of aggregated returns are typically obtained in ARCH and similar models by making the conditioned variance of successive elementary increments dependent on the past history [3, 30–32], even for more specialized

versions of this type of approach, like FIGARCH [42], a proper description of the correct scaling and multiscaling properties of aggregated increments is still an open issue.

A cornerstone achievement in statistical physics has been the formulation of the renormalization group approach to scaling [43–45]. In this approach one tries to deduce the scaling properties of a system at criticality by analyzing how coarse-graining operations, which rescale the minimal *length* at which the system is resolved, change its statistical description in terms of effective interactions or similar parameters. The scaling invariance at criticality then emerges when such changes do not occur (fixed point). In a recent publication [23], some of the present authors made the proposal that the problem of modeling the stochastic financial process on *time scales* for which a well defined scaling symmetry holds at least approximately, may be faced by inverting the logic of the standard renormalization group procedure. Given as an input the scaling properties of the aggregated increment PDF over a certain time scale, the idea is to find by fine-graining basic probabilistic rules that apply to elementary increments in order for them to be consistent with the input scaling properties [24, 34]. These rules should describe the system on time scales shorter than that of the aggregation interval, and their knowledge is regarded to be equivalent to that of the effective fixed point interactions in the standard renormalization group approach. Of course, even if properties like the martingale character of the financial process pose strong constraints, there is a degree of arbitrariness in the fine graining operation, and an important task is to show that the proposed fine-graining is plausible at the light of the relevant stylized facts.

This fine-graining, reverse renormalization group strategy for the description of market dynamics has been already exemplified in previous contributions [23, 25, 26], especially dealing with high frequency processes [35–37]. Unlike in cases for which a single time series is available, in Refs. [35–37] we focused on a particular, fixed window of the daily evolution of an asset, and extracted from the available records an ensemble of histories which have been assumed to be independent realizations of the same stochastic process. The manifest time inhomogeneous character of this process and its limited duration in time significantly simplify a modeling approach based on the above fine-graining strategy. Things become more difficult when only one realization of the process one wishes to model is available in the form of a single, long time series. This is the situation we discuss in the present work.

While a precise mathematical definition of our model is postponed to the next Section, in the present one we summarize the basic ideas behind its construction. In particular, we emphasize the inspiration by the renormalization group approach and the basic complementary role played by both endogenous and exogenous mechanisms. Another key aspect concerns the introduction of an auto-regressive dynamical scheme. In our context this

endows the endogenous mechanism with sufficiently long memory, guaranteeing at the same time strong mixing, and hence also the ergodicity of the process [48].

Let $\{X_t\}_{t=1}^{\infty}$ be a sequence of random variables representing the increments (logarithmic returns in finance) of a discrete-time stochastic process. This process possesses a simple-scaling symmetry if $X_1 + \dots + X_t$ has the same probability law as $t^H X_1$ for any t , $H > 0$ being the scaling (Hurst) exponent. If this is the case, the property

$$t^H g_t(t^H x) = g(x) \quad (1)$$

holds for the PDF g_t of the aggregated increments $X_1 + \dots + X_t$, where g is the scaling function (which also coincides with the PDF of X_1). One immediate consequence of Eq. (1) is a scaling property for the existing moments of the process:

$$\mathbb{E}[|X_1 + \dots + X_t|^q] = t^{qH} \mathbb{E}[|X_1|^q]. \quad (2)$$

A normal scaling symmetry is obtained with g Gaussian and $H = 1/2$. Anomalous scaling refers to the fact of g not being Gaussian and/or $H \neq 1/2$. Another kind of anomalous behavior for which Eq. (2) holds with an exponent H_q explicitly depending on the moment order q is called *multiscaling* and in this case H_q is also named generalized Hurst exponent [46, 47].

The simple-scaling symmetry can also be expressed in terms of characteristic functions (CF) as

$$\mathbb{E}[e^{ik(X_1 + \dots + X_t)}] = \mathbb{E}[e^{ik(t^H X_1)}], \quad (3)$$

or, equivalently, as

$$\widehat{f}_t^X(k, \dots, k) = \widehat{f}_1^X(t^H k), \quad (4)$$

where $\widehat{f}_t^X(k_1, \dots, k_t) \equiv \mathbb{E}[e^{i(k_1 X_1 + \dots + k_t X_t)}]$ is the joint CF of X_1, \dots, X_t , i.e. the Fourier transform of the joint PDF $f_t^X(x_1, \dots, x_t)$.

Aiming at constructing a model for the increments consistent with Eq. (1) for a given scaling exponent $H > 0$ and general scaling function g , we notice that the knowledge of $f_1^X = g$ combined with Eq. (4) allows us to only fix the CF \widehat{f}_t^X along the diagonal:

$$\widehat{f}_t^X(k, \dots, k) = \widehat{g}(t^H k) \equiv \int_{\mathbb{R}} dx e^{i(t^H k)x} g(x). \quad (5)$$

The basic inspiration of our approach is thus a quest for the existence of conditions implied by the presence of anomalous scaling which allow us to determine this joint CF also off-diagonal. Namely: “*Are there ways of fixing $\widehat{f}_t^X(k_1, \dots, k_t)$ such that $\widehat{f}_t^X(k, \dots, k) = \widehat{g}(t^H k)$ with g non-Gaussian and/or $H \neq 1/2$ assumed to be given?*” As a rule, when applying the renormalization group approach, one would be faced with the inverse problem: given a parametric form for \widehat{f}_t^X , or for f_t^X , one tries to fix its parameters in such a way that Eq. (4), and thus Eq. (1) with H and $g = f_1^X$ to be determined, is satisfied. This amounts to the identification of the fixed

point and is generally accomplished by operating a suitable coarse-graining operation on the description of the process. The fixed point is just an instance of the process which is left invariant under such operation. To satisfy our quest, we need to implement a plausible inversion of the coarse-graining operation in which the fixed point scaling is assumed to be known and \widehat{f}_t^X needs to be constructed. This inverse procedure is not unique in general and its plausibility needs to be tested *a posteriori*. We are thus somehow “reverting” the ordinary flux in a renormalization-group approach, as we are trying to realize a *fine-graining* procedure compatible with the existence of an anomalous fixed point scaling.

Given H and g as an input, our proposal is to set

$$\widehat{f}_t^X(k_1, \dots, k_t) = \widehat{g}\left(\sqrt{a_1^2 k_1^2 + \dots + a_t^2 k_t^2}\right) \quad (6)$$

where

$$a_i = \sqrt{i^{2H} - (i-1)^{2H}} \quad (7)$$

for any $i \in \mathbb{N}^+$, and to find conditions on g which guarantee that such a \widehat{f}_t^X is a proper CF. If this is the case, \widehat{f}_t^X is the Fourier transform of a PDF and manifestly solves Eq. (4). We thus meet with the problem of characterizing the class of scaling functions g which make the inverse Fourier transform of our trial CF a non-negative joint PDF. Fortunately, this problem is addressed by Schoenberg’s theorem [49, 50], which guarantees that Eq. (6) provides a proper CF for all t if and only if \widehat{g} is of the form

$$\widehat{g}(k) = \int_0^{\infty} d\sigma \rho(\sigma) e^{-\sigma^2 k^2/2}, \quad (8)$$

ρ being a PDF on the positive real axis. The class of scaling functions suitable for our fine-graining procedure is thus constituted by the Gaussian mixtures

$$g(x) = \int_0^{\infty} d\sigma \rho(\sigma) \mathcal{N}_{\sigma}(x), \quad (9)$$

where, here and in the following, \mathcal{N}_{σ} denotes a Gaussian PDF with mean zero and variance σ^2 . Such a class, whose elements are identified by ρ , is rich enough to allow us to account for very general anomalous scaling symmetries. The joint PDF of the variables X_t ’s provided by our inverse strategy and corresponding to g , i.e. to ρ , is then obtained by applying an inverse Fourier transform to Eq. (6) and reads

$$f_t^X(x_1, \dots, x_t) = \int_0^{\infty} d\sigma \rho(\sigma) \prod_{i=1}^t \mathcal{N}_{a_i \sigma}(x_i), \quad (10)$$

with the a_i ’s as in Eq. (7).

There are various ways in which Eq. (10) can inspire the construction of a stochastic process suitable for finance. Some possibilities have been tested in Refs. [24–26, 35, 36]. In general, the joint PDF of Eq. (10) itself

cannot describe a stationary ergodic sequence $\{X_t\}_{t=1}^\infty$, but for the problem we address here, i.e. to describe long historical time series, such features are relevant. To recover stationarity and ergodicity keeping contact with Eq. (10), we here conceive the process of the returns as separated into two components. As shown below, the manifest scaling property of the Gaussian

$$\mathcal{N}_{a\sigma}(x) = \frac{1}{a} \mathcal{N}_\sigma\left(\frac{x}{a}\right), \quad (11)$$

which holds for any $a > 0$, prompts such a separation. In the financial time series context, one is then naturally led to interpret these components as accounting for long-memory endogenous dynamical mechanisms and for the occurrence of short-memory endogenous and exogenous events, respectively.

As far as the former component is concerned, a correlated process $\{Y_t\}_{t=1}^\infty$ with memory order M is considered. Up to t equal to M , this process is characterized by the joint PDF of Eq. (10) with $a_i = 1$ for all i 's. This is a sequence of non-Gaussian, dependent random variables and at times up to M their sum satisfies a form of anomalous scaling with $H = 1/2$ and g given by Eq. (9). The introduction of a finite M of course limits the range of time for which this form of scaling is valid. This is not a problem, because empirically we know that anomalous scaling approximately holds within a finite time window. The entire process $\{Y_t\}_{t=1}^\infty$ is then obtained through an auto-regressive scheme of order M . This auto-regressive scheme is such to prevent the dynamics from stabilizing the conditional variance of Y_t 's, given the past history, to a constant value after an initial transient, thus restoring full ergodicity [24, 48]. At the same time, the conditioning effect of the previous values of the process on the future dynamical evolution is of primary importance in applications like, e.g., those related to derivative pricing [38] or volatility forecasts.

The latter component introduces a multiscaling behavior by multiplying each element of the above sequence by the corresponding factor a_t given in Eq. (7): $X_t = a_t Y_t$. In principle, these rescaling factors convey a time inhomogeneity to the increments X_t 's, a property which has been exploited in the modeling of ensembles of histories [35–37]. However, a proper randomization of the time argument of the a_t 's restores the stationarity of the X_t 's, making them suitable for describing single time series whose statistical properties are thought to be independent of time [10]. This randomization, which is obtained by the introduction of a short-memory process, is regarded as mimicking the effects on market evolution of both short-memory endogenous random factors and external inputs of information or changing conditions, thus conferring also an exogenous character to this second component. The first component, which is responsible for the volatility clustering phenomenon thanks to its possible long dynamical memory M , is then interpreted as the long-memory endogenous part. In order to have a simple intuition of the returns' compound process, we

may sketch a comparison with electronics and telecommunications regarding the long-memory component as a carrier signal, which is modulated by the short-memory one, playing thus the role of a modulating signal.

As we shall review in the Paper, and show in the Supplementary Material [40], relevant properties of the model, like its multiscaling and the power-law decay of non-linear autocorrelations over finite time horizons, are determined by the short-memory component. We stress that when combining the long-memory and short-memory processes, together with simple scaling features also the direct link between the Hurst exponent and the exponent H entering in Eq. (7) is lost. For this reason, in the following we will denote by D , instead of H , the parameter involved in the definition of the model [See Eq. (19) below].

III. MODEL DEFINITION

On the basis of the background material elaborated in the previous Section, here we precisely define our stochastic process of the increments. Such a process $\{X_t\}_{t=1}^\infty$ is obtained as the product of an endogenous auto-regressive component $\{Y_t\}_{t=1}^\infty$ and a rescaling, or modulating, factor $\{a_{I_t}\}_{t=1}^\infty$, where $\{I_t\}_{t=1}^\infty$ is a discrete Markovian random time independent of $\{Y_t\}_{t=1}^\infty$, and $\{a_i\}_{i=1}^\infty$ is a positive sequence:

$$X_t \equiv a_{I_t} Y_t. \quad (12)$$

The stochastic process $\{Y_t\}_{t=1}^\infty$ is a Markov process taking real values with memory $M > 0$. It is defined, through its PDF's, by the following scheme:

$$f_t^Y(y_1, \dots, y_t) \equiv \varphi_t(y_1, \dots, y_t) \quad (13)$$

if $t = 1, 2, \dots, M$, and

$$f_t^Y(y_1, \dots, y_t) \equiv \frac{\varphi_{M+1}(y_{t-M}, \dots, y_t)}{\varphi_M(y_{t-M}, \dots, y_{t-1})} \cdot f_{t-1}^Y(y_1, \dots, y_{t-1}) \quad (14)$$

if $t > M$. Here, the PDF's φ_t are given by

$$\varphi_t(y_1, \dots, y_t) \equiv \int_0^\infty d\sigma \rho(\sigma) \prod_{n=1}^t \mathcal{N}_\sigma(y_n). \quad (15)$$

The process $\{I_t\}_{t=1}^\infty$ is a Markov chain of order 1 valued in \mathbb{N}^+ . The memory order 1 of this sequence, to be compared with the memory order M of the above one, justifies our convention of referring the two components as “short-memory” and “long-memory”, respectively. The chain $\{I_t\}_{t=1}^\infty$ is defined by the initial condition

$$\mathbb{P}[I_1 = i] \equiv \nu(1 - \nu)^{i-1} \quad (16)$$

and by the transition probabilities

$$\mathbb{P}[I_{t+1} = i | I_t = j] \equiv \begin{cases} \nu & \text{if } i = 1; \\ 1 - \nu & \text{if } i = j + 1; \\ 0 & \text{otherwise.} \end{cases} \quad (17)$$

In words, we are stating that at time $t + 1$ there is a “time-reset” or “restart” ($I_{t+1} = 1$) with probability $\nu > 0$, whereas with probability $1 - \nu$ time flows normally ($I_{t+1} = I_t + 1$). For notational simplicity we set $\pi(i) \equiv \mathbb{P}[I_1 = i]$ and we collect the transition probabilities into a stochastic matrix with entries $W(i, j) \equiv \mathbb{P}[I_{t+1} = i | I_t = j]$. We point out that our choice of π corresponds to the invariant distribution of W , with the consequence that $\{I_t\}_{t=1}^\infty$ turns out to be a stationary process:

$$\sum_{j=1}^{\infty} W(i, j)\pi(j) = \pi(i). \quad (18)$$

It should be stressed that here we assume that $\{Y_t\}_{t=1}^\infty$ and $\{I_t\}_{t=1}^\infty$ are independent in favor of an initial simplicity. As a consequence, the present model results in a Markov-switching model where, by definition, the switching mechanism between different regimes is controlled by an unobservable state variable that follows a first-order Markov chain. In Section VIII we shall then hint at the possibility of making the random time $\{I_t\}_{t=1}^\infty$ dependent on $\{Y_t\}_{t=1}^\infty$.

Finally, $\{a_i\}_{i=1}^\infty$ is a positive sequence where, without loss of generality, we can set $a_1 = 1$. In analogy with the previous Section, we assume a factor a_i of the form

$$a_i = \sqrt{i^{2D} - (i-1)^{2D}} \quad (19)$$

with $D > 0$. The relation between the Hurst exponent and the model parameter D will be addressed in what follows. For the moment, let us point out that the sequence a_i is identically equal to 1 if $D = 1/2$ while monotonically decays to zero or diverges if $D < 1/2$ or $D > 1/2$, respectively. For financial applications, the instance $D < 1/2$ appears to be the interesting one and, since $\lim_{i \rightarrow \infty} i^{1/2-D} a_i = \sqrt{2D}$, the decay of the rescaling factor is of power-law type. However, in principle other choices for the functional form of $\{a_i\}_{i=1}^\infty$ are possible and could be introduced for further extensions and applications of the model.

The endogenous process $\{Y_t\}_{t=1}^\infty$ recalls the ARCH construction of order M [30] because the conditional PDF of the current Y_t , given the past history, depends on the previous outcomes only through the sum of the squares of the latest M ones, as one can easily recognize. As a matter of fact, $\{Y_t\}_{t=1}^\infty$ becomes a genuine ARCH process if the function ρ is properly chosen, as we shall show in a moment. In general, the basic difference with respect to an ARCH process is that here the whole conditional PDF of Y_t , and not only its variance, changes with time. In spite of this, the process $\{Y_t\}_{t=1}^\infty$ is identified by a small number of parameters independently of the order M . Indeed, besides M , the parameters associated to $\{Y_t\}_{t=1}^\infty$ are only those related to ρ . As we discuss below, satisfactory parametrizations of ρ for financial time series require just two parameters. This must be contrasted with the fact that in realistic ARCH models the number of parameters can proliferate with the memory, easily becoming

of the order of several tens [3]. Such a synthetic result, which we believe to be a most interesting innovative feature of $\{Y_t\}_{t=1}^\infty$, is made possible by the exploitation of the scaling symmetry embodied in Eqs. (13–15).

A most practical choice for ρ is one which allows us to explicitly perform the integration over σ in Eq. (15). Indeed, we notice that weighing σ^2 according to an inverse-gamma distribution is the way to reach this goal. Furthermore, in the context of financial modeling, this prescription is in line with the rather common belief that the distribution of the square of the empirical returns can be modeled as an inverse-gamma distribution [25, 53, 54]. This ρ is identified by two parameters, α and β governing its form and the scale of fluctuations, respectively, and reads

$$\rho(\sigma) = \frac{2^{1-\frac{\alpha}{2}}}{\Gamma(\frac{\alpha}{2})} \frac{\beta^\alpha}{\sigma^{\alpha+1}} e^{-\frac{\beta^2}{2\sigma^2}}, \quad (20)$$

where Γ denotes the Euler’s gamma function. Interestingly, making this choice within the model, the endogenous component $\{Y_t\}_{t=1}^\infty$ becomes a true ARCH process of order M with Student’s t-distributed return residuals, as anticipated above. Indeed, in the Supplementary Material [40] we prove that if ρ is given by Eq. (20), then we can reformulate our model as $X_t = a_{I_t} Y_t$ with

$$Y_t = \begin{cases} \beta \cdot Z_1 & \text{if } t = 1; \\ \sqrt{\beta^2 + \sum_{n=1}^{\min\{t-1, M\}} Y_{t-n}^2} \cdot Z_t & \text{if } t > 1, \end{cases} \quad (21)$$

and the return residual process $\{Z_t\}_{t=1}^\infty$ amounting to a sequence of independent Student’s t-distributed variables:

$$f_t^Z(z_1, \dots, z_t) = \prod_{n=1}^t \frac{\Gamma(\frac{\alpha_n+1}{2})}{\sqrt{\pi} \Gamma(\frac{\alpha_n}{2})} (1 + z_n^2)^{-\frac{\alpha_n+1}{2}} \quad (22)$$

with $\alpha_n \equiv \alpha + \min\{n-1, M\}$. It is also worth noticing that the Markov-switching character of the volatility, introduced by the process $\{a_{I_t}\}_{t=1}^\infty$, reconciles this particular instance of our model with the SWARCH category proposed by Hamilton and Susmel [55]. The only difference, apart from dealing with an infinite number of regimes corresponding to the infinite possible values taken by I_t , is that these regimes never persist for more than one time step. We stress however that besides M only two parameters, α and β , are here needed to completely specify $\{Y_t\}_{t=1}^\infty$. This typically applies also to other possible parametrizations of ρ , not related to the inverse-gamma distribution.

The $\{a_{I_t}\}_{t=1}^\infty$ component entails our model with two further parameters, i.e. ν establishing the frequency of occurrence of the “time restarts”, and the exponent D defining the modulating factor $\{a_i\}_{i=1}^\infty$. In summary, the model is thus typically identified by 5 parameters, three related to the long-memory and two to the short-memory components. The general fact that both $\{Y_t\}_{t=1}^\infty$ and $\{a_{I_t}\}_{t=1}^\infty$ are *hidden processes*, not separately detectable,

complicates the effectiveness of a parameter calibration protocol. However, as discussed below, analytical features of the model allow us to identify moment optimization procedures that guarantee, for sufficiently long time-series, proper determination of the input parameters.

In the next Section we clarify in details up to what extent the scaling symmetry is preserved by the process $\{X_t\}_{t=1}^{\infty}$. For the moment we point out that the contact with the ARCH and Markov-switching models' literature is particularly interesting. Indeed, thanks to our general results below it sheds some light on how to obtain anomalous scaling properties in auto-regressive models on limited temporal horizons [22].

IV. MODEL PROPERTIES

A number of properties of our model are independent of the choice of the function ρ and can be analytically investigated. Here we briefly review these properties referring to the Supplementary Material [40] for detailed derivations.

A. Joint PDF and stationarity

For any $t \geq 1$ the joint PDF of X_1, \dots, X_t is given by the formula

$$f_t^X(x_1, \dots, x_t) = \sum_{i_1=1}^{\infty} \cdots \sum_{i_t=1}^{\infty} \prod_{n=1}^{t-1} W(i_{n+1}, i_n) \pi(i_1) \cdot \frac{f_t^Y(x_1/a_{i_1}, \dots, x_t/a_{i_t})}{a_{i_1} \cdots a_{i_t}}. \quad (23)$$

Since f_t^Y is defined via mixtures of centered Gaussian variables, Eq. (15), we realize immediately that the conditional expectation of X_t , given the past history, vanishes. The process $\{X_t\}_{t=1}^{\infty}$ is thus a martingale difference sequence, reflecting the efficient market hypothesis [56, 57]. Moreover, the structure of f_t^X shows that the observed process cannot retain the Markov property characterizing both $\{Y_t\}_{t=1}^{\infty}$ and $\{a_{I_t}\}_{t=1}^{\infty}$, with the consequence that its future evolution always depends on all past events. This feature reflects the impossibility of directly detecting from the examination of $\{X_t\}_{t=1}^{\infty}$ the random time $\{I_t\}_{t=1}^{\infty}$. More importantly, the latter fact makes a maximum-likelihood estimation of the model parameters very difficult because of the too onerous computational work needed. Thus, one is forced to refer to some moment optimization procedure for settling this issue. For this reason, in the next Section we shall propose a simple implementation of a generalized method of moments. A procedure to identify the most probable time restarts by means of the calibrated model, valuable for some applications like, e.g., in option pricing, will be also discussed in Section VII.

A remarkable feature of the joint PDF f_t^X is that it does not explicitly depend on the memory range M at

short time scales. Indeed, when $t \leq M + 1$ from Eqs. (4) and (13) we have [notice that Eq. (14) gives $f_{M+1}^Y = \varphi_{M+1}$]

$$f_t^X(x_1, \dots, x_t) = \sum_{i_1=1}^{\infty} \cdots \sum_{i_t=1}^{\infty} \prod_{n=1}^{t-1} W(i_{n+1}, i_n) \pi(i_1) \cdot \int_0^{\infty} d\sigma \rho(\sigma) \prod_{n=1}^t \mathcal{N}_{a_{i_n} \sigma}(x_n). \quad (24)$$

This fact implies that models with different memory orders M and $M' > M$, and the same other parameters, cannot be distinguished by looking at their features at times shorter than or equal to $M + 1$. Observe also that the Gaussian mixture structure provided by our fine-graining strategy and the random nature of the factor redefining the typical magnitude of the fluctuations is particularly clear in Eq. (24).

Our process is strictly stationary, meaning that (X_n, \dots, X_{n+t-1}) is distributed as (X_1, \dots, X_t) for any $n \geq 1$ and $t \geq 1$. This property directly follows from the fact that $\{Y_t\}_{t=1}^{\infty}$ and $\{I_t\}_{t=1}^{\infty}$ are both stationary processes and, in particular, tells us that Eqs. (4) and (24) give the PDF of any string of t consecutive variables extracted from $\{X_t\}_{t=1}^{\infty}$. We stress that stationarity is a basic assumption in time series analysis, when one is forced to reconstruct the underlying stochastic process on the basis of a single, possibly long, time series.

We also point out that the long-memory endogenous component $\{Y_t\}_{t=1}^{\infty}$ is not only a stationary sequence, but even a reversible one: the law of $(Y_t, Y_{t-1}, \dots, Y_1)$ is the same as the law of $(Y_1, \dots, Y_{t-1}, Y_t)$ for any $t \geq 1$. In contrast, the observed process $\{X_t\}_{t=1}^{\infty}$ is not reversible, being such time-reversal symmetry broken by the short-memory component. In Section VI we shall better analyze this feature of the model, attempting to quantify the time-reversal asymmetry of $\{X_t\}_{t=1}^{\infty}$.

The single-variable PDF, which is the same for any X_t thanks to stationarity, is obtained by setting $t = 1$ in Eq. (24) and explicitly reads

$$f_1^X(x) = \sum_{i=1}^{\infty} \nu(1-\nu)^{i-1} \int_0^{\infty} d\sigma \rho(\sigma) \mathcal{N}_{a_i \sigma}(x). \quad (25)$$

The mixture of Gaussian densities with different width can endow this PDF with power law tails, as observed for financial assets [10]. Specifically, when $\rho(\sigma)$ decays as the power-law $\sigma^{-\alpha-1}$ for large σ , f_1^X becomes a fat-tailed distribution with the same tail index α . Thus, for example choosing ρ as in Eq. (20) we have $\lim_{x \rightarrow \infty} |x|^{\alpha+1} f_1^X(x) = c$ with

$$c \equiv \frac{\beta^\alpha \Gamma(\frac{\alpha+1}{2})}{\sqrt{\pi} \Gamma(\frac{\alpha}{2})} \sum_{i=1}^{\infty} a_i^\alpha \nu(1-\nu)^{i-1} < \infty, \quad (26)$$

and the above form parameter α controls the tails of the PDF of the X_t 's as long as ν is finite. It is worth noticing that, even if the above condition on ρ is necessary

for having fat tails in a strict asymptotic sense, there is the possibility of approximately realizing such a feature for returns in empirically accessible ranges by only considering rare enough time restarts. As explained in the Supplementary Material [40], indeed, assuming $\{a_i\}_{i=1}^{\infty}$ given by Eq. (19) with $D < 1/2$, and properly rescaling ρ in order to avoid f_1^X to concentrate around zero in the small- ν limit, in general the single-variable PDF displays fat tails with index $2/(1-2D)$ when the restart probability ν approaches zero. Of course, with $\rho(\sigma)$ behaving as $\sigma^{-\alpha-1}$ for large σ and $\alpha < 2/(1-2D)$, the tail index is determined by α even in the rare-restart limit. In practice, when dealing with small values of ν the empirically-accessible power law exponent of f_1^X depends on all α , ν , and D . This fact, and the uncertainty affecting the empirical estimate of such exponent [10], lead us to a calibration protocol (See below) which is not based on matching the effective power law tails of f_1^X .

Since we have here stated the stationarity of our model, we also mention that strong mixing properties can be proved under mild assumptions on the function ρ [48]. These mixing properties entail ergodicity, which justifies the comparison between empirical long time averages and theoretical ensemble expectations. They also imply the validity of the central limit theorem, to which we appeal for discussing scaling features of aggregated returns on the long time horizon under, basically, the only hypothesis that the second order moment of the elementary increments is finite. Stating precisely these results and discussing their proof however requires a more rigorous setting [48] which is beyond the scope of the present Paper. The ergodicity has also been numerically verified on the basis of model-based simulations.

B. Scaling features

Scaling features of $\{X_t\}_{t=1}^{\infty}$ are at the heart of our approach and two different scaling regimes, corresponding to the empirical evidence found for financial assets [47, 51, 52], can be identified within the present model: one is an effective multiscaling regime, which is most easily discussed in analytical terms for $t \leq M + 1$, and the other is an asymptotic Gaussian simple-scaling scenario, which prevails for $t \gg M$ as a consequence of the central limit theorem mentioned above [48]. We focus here on the former, which is directly relevant for applications in finance.

The moment time-dependence of the aggregated return $X_1 + \dots + X_t$ is only ruled by the short-memory component if $t \leq M + 1$, since Eq. (24) enables one to demonstrate [40] that in such a case

$$\begin{aligned} m_q^X(t) &\equiv \frac{\mathbb{E}[|X_1 + \dots + X_t|^q]}{\mathbb{E}[|X_1|^q]} \\ &= \frac{\mathbb{E}[(a_{I_1}^2 + \dots + a_{I_t}^2)^{\frac{q}{2}}]}{\mathbb{E}[a_{I_1}^q]}. \end{aligned} \quad (27)$$

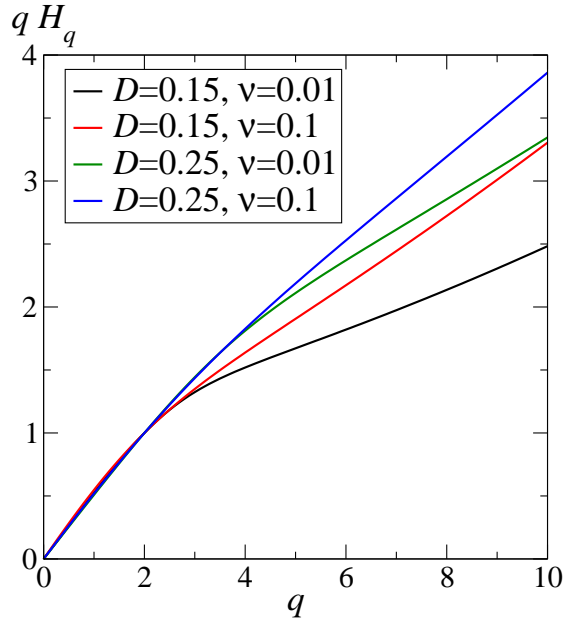


FIG. 1: Model multiscaling behavior for $1 \leq t \leq 31$ and $M \geq 30$. The couple (D, ν) determines the behavior.

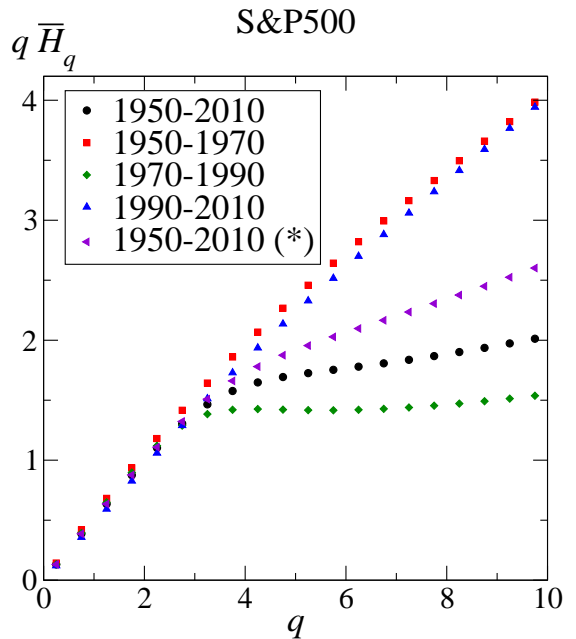


FIG. 2: Simple- ($q \lesssim 3$) and multi- ($q \gtrsim 3$) scaling behavior of S&P500 (log) returns PDF, analyzed for t from 1 day to 2 months in the years 1950-2010. Notice the strong dependence of multiscaling features on the specific sample. In particular, data marked with (*) refer to the full interval 1950-2010 with an artificial alteration of a single data: a reduction of 20% of the strongest fluctuation.

Notice that the r.h.s. of Eq. (27) is well defined for any q . If the X_t 's PDF's are endowed with fat tails, this is not true for the l.h.s. of the same equation. When $D < 1/2$ and not too small, effective scaling properties of the model follow from the fact that m_q^X , although apparently a rather complex function of the time, is well approximated by the power $t^{q H_q}$ for $t \leq M + 1$ [40]. The generalized Hurst-like exponent H_q can be computed using a least squares method over time. Referring for instance to a temporal window extending up to $t = 31$ and adopting a memory order $M \geq 30$, Fig. 1 displays H_q for different pairs of D and ν values. The exponent H_q stays close to $1/2$ for low orders q up to about $2/(1 - 2D)$, denoting an initial simple-scaling regime. It recovers a dependence on q for larger moment orders, manifesting a multiscaling behavior. A sharp result is found in the limit of small ν , where $H_q = 1/2$ for $q \leq 2/(1 - 2D)$ [40].

In the perspective of a comparison of our model with data, a remark on the scaling features of empirical financial data is in order (See also [25]). While the simple-scaling behavior at low q is a stable and robust empirical evidence, multiscaling features occurring at larger q are sensibly dependent on the time series sample, for series of a length comparable with that at our disposal for the S&P500 index. We report this observation in Fig. 2 with respect to the S&P500 daily time series. The empirical exponent \overline{H}_q is here obtained from the time-average estimation of m_q^X , as computed in the next Section. In turn, from the modeling point of view, the multiscaling region in the moment order axis mostly overlaps the non-existing moment region when fat-tailed distributions are involved.

C. Volatility autocorrelation

In view of financial applications, the volatility autocorrelation of order q can be introduced as the autocorrelation function of the process $\{|X_t|^q\}_{t=1}^\infty$:

$$r_q^X(t) \equiv \frac{\mathbb{E}[|X_1|^q |X_t|^q] - \mathbb{E}[|X_1|^q]^2}{\mathbb{E}[|X_1|^{2q}] - \mathbb{E}[|X_1|^q]^2}. \quad (28)$$

Again, this autocorrelation is easily investigated for $t \leq M + 1$, where the Markov-switching component alone determines its decay. Indeed, thanks to the independence of the processes $\{Y_t\}_{t=1}^\infty$ and $\{I_t\}_{t=1}^\infty$, $r_q^X(t)$ can be rewritten as [40] $r_q^X(t) = u_q + v_q r_q^{a_I}(t)$ for $2 \leq t \leq M + 1$, while $r_q^X(1) = 1$. Here, $r_q^{a_I}$ is the autocorrelation of $\{a_{I_t}^q\}_{t=1}^\infty$, and u_q, v_q are two time-independent coefficients whose explicit expression is provided in the Supplementary Material [40]. We thus see that the time dependence of r_q^X comes from $r_q^{a_I}$ at short time scales $t \leq M + 1$. Interestingly, for q small enough, the smaller the restart probability ν , the more correlations get persistent: when ν approaches zero, we find $r_q^{a_I}(t) = 1$ for any t if $q \leq 1/(1 - 2D)$. Notice that this last threshold for the moment order q is now half of that previously discussed for the simple-scaling behavior.

While the initial decay of the volatility autocorrelation r_q^X is strongly dependent on the parameter setting, in particular through the ratio u_q/v_q , on time scales much larger than M , r_q^X decays exponentially fast, due to the strong mixing properties of our model [48]. In the Supplementary Material [40] we show that this is indeed the case focusing on the function ρ given by Eq. (20) and the instance $q = 2$, for which the correlation decay rate can be explicitly computed.

We conclude the Section with a remark concerning our convention of referring to ‘‘long-memory’’ and ‘‘short-memory’’ processes, which contrasts with some common use in the econometric literature. Indeed, within this literature a process is said to possess long memory if the autocorrelation is not summable in time [58]. The asymptotic exponential decay of $r_1^Y(t)$ provided by our model [40] entails that the above sum is finite also for the process $\{Y_t\}_{t=1}^\infty$. However, our convention stresses the different structure of the two components.

V. MODEL CALIBRATION

An important issue for the application of a model to time series analysis is the implementation of efficient calibration protocols, capable of identifying the model parameters which most effectively reproduce a specific empirical evidence. As anticipated, the inclusion of both a long-memory and a short-memory part in our model complicates the calibration procedure, because the two components cannot be easily resolved along an empirical time series. In order to overcome this difficulty, we devise here a method based on the comparison between empirical and theoretical moments, drawing on the generalized method of moments [59] and taking advantage of the analytical structure of our model.

With the relatively limited amount of daily historical data available for financial assets, the identification of the model parameters is affected by large uncertainties. Since our memory parameter M establishes the time horizon over which the long-memory endogenous dynamical dependence operates, we can choose to fix it on the basis of the time scale associated with the specific application of interest. Given M , we thus optimally exploit the simple analytical structure within the time window $1 \leq t \leq M$ for the calibration of the remaining parameters. In order to present the procedure and to test our model on real data, we refer here and in the following to the advantageous function ρ introduced in Section III by Eq. (20). Once M is fixed, the further parameters to be estimated are four: the exponent $D > 0$, the restart probability $0 < \nu \leq 1$, and the parameters $\alpha > 0$ and $\beta > 0$ identifying ρ . For simplicity, we collect the first three of them into the vector $\theta \equiv (D, \nu, \alpha)$ and we denote by Θ its feasible range. The parameter β plays a minor role in the model since we only need it to fix the scale of X_t 's fluctuations.

Given a time series $\{\overline{x}_t\}_{t=1}^T$ with empirical mean zero,

our calibration protocol is based on the idea of better reproducing, within the model, its scaling and autocorrelation features on times up to M . Thus, in a least square framework, we choose those parameters which minimize the distance between the theoretical $m_q^X(t)$ and $r_q^X(t)$, defined by Eqs. (27) and (28) respectively, and the corresponding empirical estimations $\overline{m}_q^X(t)$ and $\overline{r}_q^X(t)$ in the window $1 \leq t \leq M$. Such empirical estimations are obtained via time averages over the available series. To illustrate the computation, for instance we get $\overline{m}_q^X(t)$ as $\mathcal{M}_q(t)/\mathcal{M}_q(1)$ with

$$\mathcal{M}_q(t) \equiv \frac{1}{T+1-t} \sum_{n=0}^{T-t} |\overline{x}_{n+1} + \dots + \overline{x}_{n+t}|^q. \quad (29)$$

We recall that the comparison between empirical time averages and theoretical ensemble expectations is justified by the ergodicity of our process [48].

Being properly normalized, m_q^X and r_q^X do not depend on the scale parameter β . Denoting by \mathcal{Q} the set of the moment orders we consider for the calibration purposes, our parameter estimation $\overline{\theta} \equiv (\overline{D}, \overline{\nu}, \overline{\alpha})$ results thus to be

$$\overline{\theta} = \arg \min_{\theta \in \Theta} \left\{ \sum_{q \in \mathcal{Q}} \sum_{t=1}^M \left[\frac{m_q^X(\theta; t) - \overline{m}_q^X(t)}{m_q^X(\theta; t)} \right]^2 + \sum_{q \in \mathcal{Q}} \sum_{t=1}^M \left[\frac{r_q^X(\theta; t) - \overline{r}_q^X(t)}{r_q^X(\theta; t)} \right]^2 \right\}, \quad (30)$$

where the dependence of m_q^X and r_q^X on θ is explicitly indicated. We have directly checked that this calibration procedure precisely recovers the input parameters when applied to sufficiently long time series simulated through the model.

We close the calibration protocol providing a way of estimating the parameter β . Once \overline{D} , $\overline{\nu}$, and $\overline{\alpha}$ have been obtained, we can evaluate β by optimizing with respect to $e_q^X \equiv \mathbb{E}[|X_1|^q]$, where D , ν , and α are set equal to \overline{D} , $\overline{\nu}$, and $\overline{\alpha}$ respectively. Making explicit the dependence of e_q^X on β , the relationship $e_q^X(\beta) = e_q^X(1)\beta^q$ is rather evident. If \overline{e}_q^X denotes the empirical counterpart of e_q^X , we then get our estimation $\overline{\beta}$ of β through the formula

$$\overline{\beta} = \arg \min_{\beta \in (0, \infty)} \left\{ \sum_{q \in \mathcal{Q}} \left[\frac{e_q^X(\beta) - \overline{e}_q^X}{e_q^X(\beta)} \right]^2 \right\}. \quad (31)$$

Aiming at reducing the computational load of the parameter estimations, in the present Paper we work out calibration with the moment order $q = 1$ only: $\mathcal{Q} = \{1\}$. Fig. 3a and 4a report the result of this protocol applied to the logarithmic increments of the daily closures of S&P500 from January 1st 1950 to December 31st 2010. We set $\overline{x}_t \equiv \ln \overline{s}_t - \ln \overline{s}_{t-1} - \mu$ for $t = 1, \dots, T$, being $T = 15385$ and $\{\overline{s}_t\}_{t=0}^T$ the considered S&P500 time series. The value of the drift μ is such that $\sum_{t=1}^T \overline{x}_t = 0$. In compliance with an application we are developing to

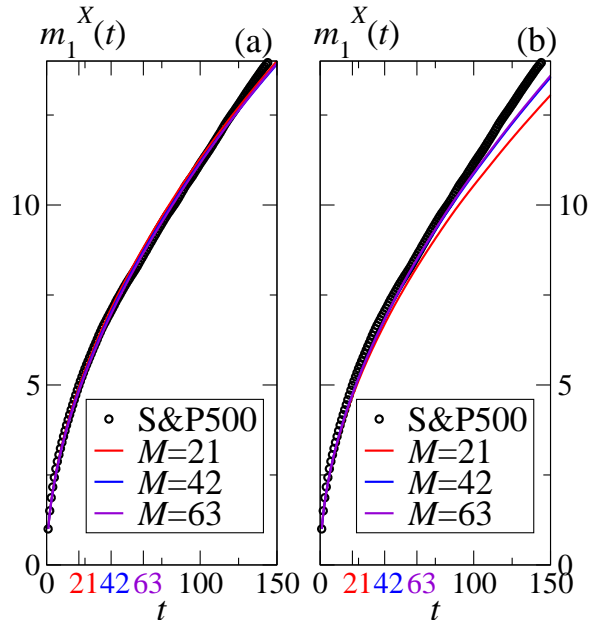


FIG. 3: Calibration outcome in terms of the scaling indicator m_1^X for different values of M , also reported in the abscissa with different colors. In (a) the model with ρ given by Eq. (20); in (b) the null model.

derivative pricing [36], we have chosen $M = 21$ (the operating market days in one month) yielding $(\overline{D}, \overline{\nu}, \overline{\alpha}, \overline{\beta}) = (0.21, 0.030, 4.0, 0.04)$, $M = 42$ (two months) giving $(\overline{D}, \overline{\nu}, \overline{\alpha}, \overline{\beta}) = (0.19, 0.011, 4.5, 0.07)$, and $M = 63$ (three months) for which $(\overline{D}, \overline{\nu}, \overline{\alpha}, \overline{\beta}) = (0.16, 0.004, 5.5, 0.14)$. Notice how the calibrated model fits the S&P500 scaling features and the volatility autocorrelation well beyond M in the case of two and three months, whereas one month does not seem to be enough to get the correct decay as soon as t is larger than 21.

VI. COMPARISON WITH S&P500 INDEX AND NULL HYPOTHESIS

In order to put into context the performance of our model and to probe the role of the memory M , here we consider, as the null hypothesis, a limit version in which σ is kept fixed to a constant value σ_0 [$\rho(\sigma) = \delta(\sigma - \sigma_0)$], which turns out to be the scale parameter. From Eq. (15) we get that this prescription replaces the autoregressive component with a sequence of independent normal variables, preventing the parameter M from playing any role [71]. Even if the null model has no endogenous memory, for the sake of comparison we estimate its parameters (first D and ν , and later σ_0) by means of the procedure outlined in the previous Section and with the same values of M and q used for the model characterized by the function ρ of Eq. (20), which we name here “the complete model”. Figs. 3b and 4b

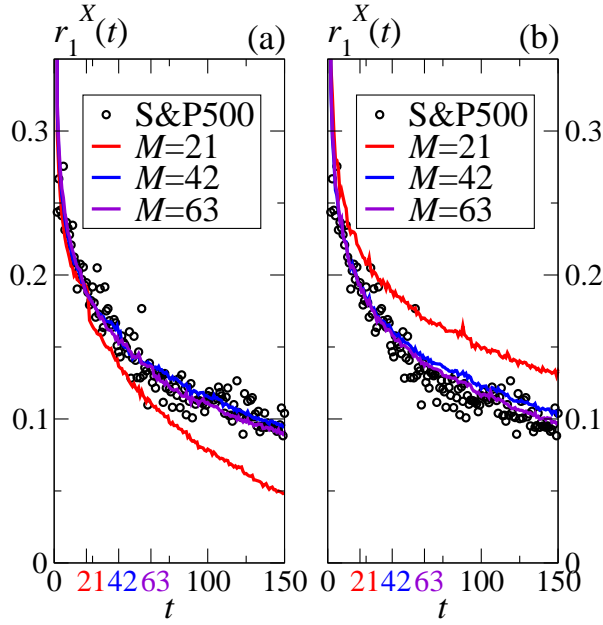


FIG. 4: Calibration outcome in terms of the volatility autocorrelation r_1^X . In (a) the model with ρ given by Eq. (20); in (b) the null model.

show the outcome of the calibration protocol, which gives the following results: $(\bar{D}, \bar{\nu}, \bar{\sigma}_0) = (0.05, 0.0001, 1.01)$ for $M = 21$, $(\bar{D}, \bar{\nu}, \bar{\sigma}_0) = (0.06, 0.0002, 0.62)$ for $M = 42$, and $(\bar{D}, \bar{\nu}, \bar{\sigma}_0) = (0.07, 0.0003, 0.45)$ when $M = 63$. The figures indicate that calibration is slightly less successful for the null model than for the complete one.

The unconditional return PDF of the S&P500 is very well reproduced by both the complete and the null calibrated models, both in the central part and in the tails. We realize this fact by an inspection of the linear and log plots of f_1^X in Figs. 5 and 6 respectively. While the function ρ defined by Eq. (20) endows the complete model with fat tails, setting $\sigma = \sigma_0$ prevents the null model from recovering such a feature from a strict mathematical standpoint. However, in Section IV A we mentioned that with a small enough value of the restart probability ν one recovers an effective fat tails scenario when $D < 1/2$. This circumstance explains why the null model reproduces the empirical fat tails thanks to an estimated value of ν which is one or two orders of magnitude smaller than the corresponding value for the complete model. The drawback is that a very small restart probability entails very rare but high and strongly time-asymmetric volatility bursts in the typical trajectories of the model, which are not observed in the historical series. Indeed, Fig. 7b, showing the comparison of typical simulated realizations of the benchmark model with the S&P500 time series, reports the discrepancy between the S&P500 and the null model paths, where one can immediately identify the time restarts. In contrast, once the auto-regressive component retains the memory of the previous returns,

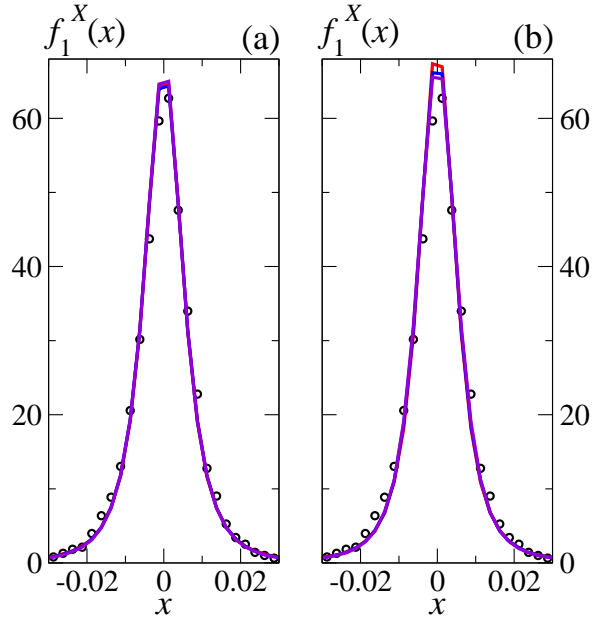


FIG. 5: Single-variable PDF comparison between S&P500 and calibrated complete model (a), and between S&P500 and the null model (b) in linear scale. Symbols and lines color code is as in the previous plots.

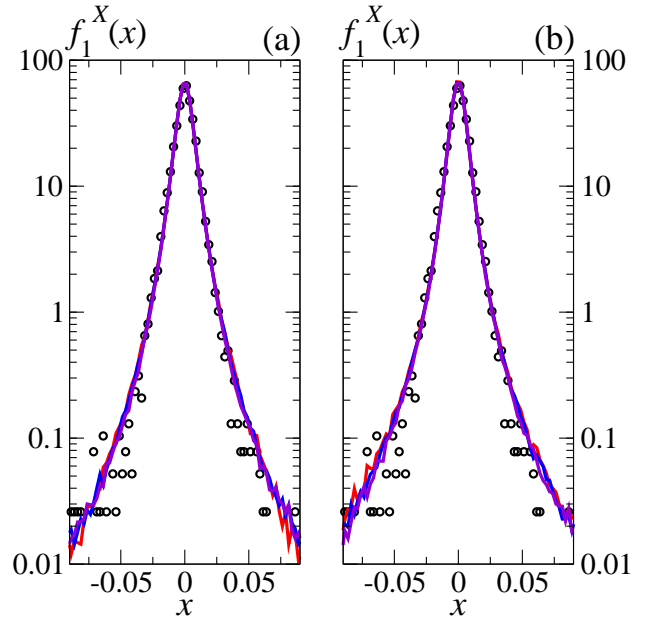


FIG. 6: Single-variable PDF comparison between S&P500 and calibrated complete model (a), and between S&P500 and the null model (b) in log scale. Symbols and lines color code is as in the previous plots.

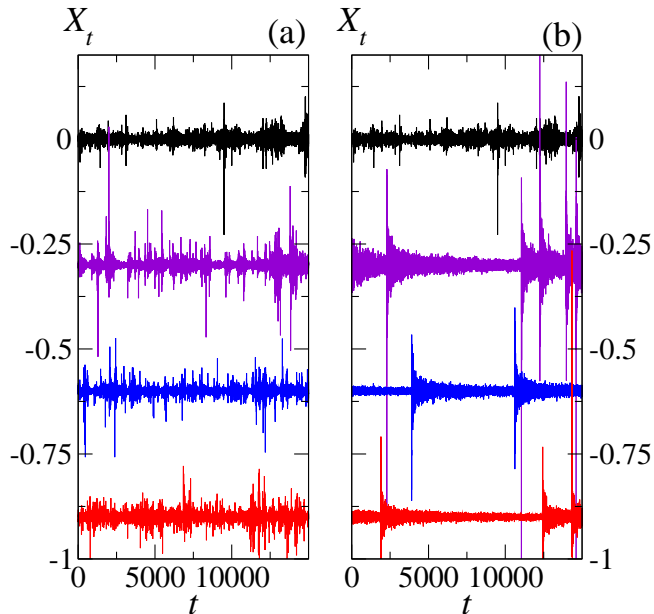


FIG. 7: Time series comparison between S&P500 (black) and complete model (a), and between S&P500 (black) and the null model (b). To facilitate the inspection, model time series are shifted by -0.3 ($M = 63$), -0.6 ($M = 42$), and -0.9 ($M = 21$).

the combined effect of more frequent restarts and of the volatility clustering phenomenon produces typical trajectories which are pretty similar to the historical S&P500, as shown in Fig. 7a where the above comparison is proposed for the complete model. Notice that restart events become here much harder to identify.

In order to recover the role of the exponent D , in Figs. 8a and 8b we also compare the aggregated return scaling features of the calibrated models with those of the S&P500 series. While, as anticipated in Fig. 2, the empirical multiscaling regime is very erratic and dependent on single extreme events, the simple-scaling behavior ($\bar{H}_q \simeq 1/2$) up to $q \simeq 3$ seems a stable feature of the S&P500. On the other hand, in Section IV B we noticed that our model predicts that the latter extends up to $q = 2/(1 - 2D)$ at low values of ν when $D < 1/2$, irrespective of the function ρ . The complete model provides $2/(1 - 2\bar{D}) = 3.4$ for the calibration with $M = 21$, $2/(1 - 2\bar{D}) = 3.2$ for $M = 42$, and $2/(1 - 2\bar{D}) = 2.9$ if $M = 63$, therefore showing a qualitative agreement with the empirical evidence. The same cannot be said for the null model, which gives $2/(1 - 2\bar{D})$ close to 2 for all the three calibrations.

Financial time series are reported to break time-reversal invariance, not only in terms of return-volatility correlation properties (e.g., the leverage effect [7, 39]), but also in terms of volatility-volatility correlations [60]. Although in the form discussed so far our model cannot explain the former (which is an odd-even correlation), it

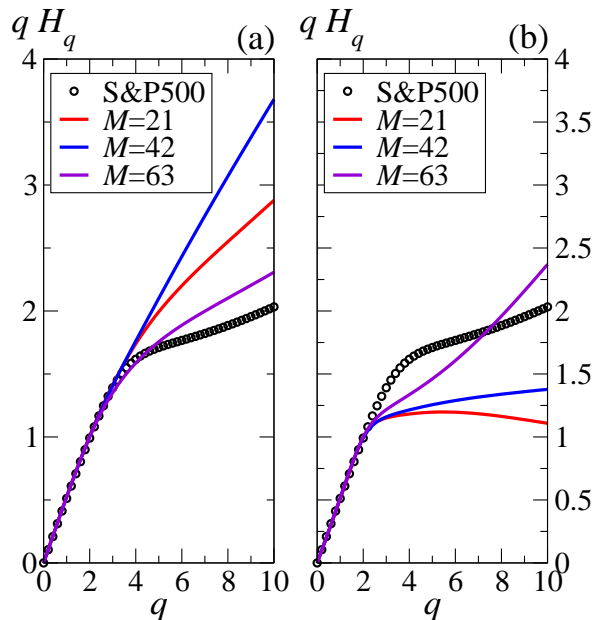


FIG. 8: Multiscaling comparison between the S&P500 and the complete model (a), and between the S&P500 and the null model (b).

can account for the latter since, as we have already mentioned in Section IV A, the Markov-switching component breaks the temporal symmetry through the mechanism of time restarts. We thus conclude this Section considering an even-even correlation, specifically the historical versus realized volatility correlation [18–20, 25, 60], and assessing an asymmetry between the past and the future for the calibrated complete model. In Section VIII we shall discuss how to improve the present model in order to also take into account the leverage effect.

Consider two consecutive time windows, named “historical” and “realized”, of width $t_h \geq 1$ and $t_r \geq 1$, respectively. The associated “historical volatility” $S_{t_h}^h$ and “realized volatility” $S_{t_r}^r$ are defined as the random variables

$$S_{t_h}^h \equiv \sqrt{\frac{1}{t_h} \sum_{t=1}^{t_h} X_t^2} \quad (32)$$

and

$$S_{t_r}^r \equiv \sqrt{\frac{1}{t_r} \sum_{t=1}^{t_r} X_{t_h+t}^2}. \quad (33)$$

For a reversible process, the correlation between past and future volatilities [61], namely

$$\chi(t_h, t_r) \equiv \frac{\mathbb{E}[S_{t_h}^h S_{t_r}^r] - \mathbb{E}[S_{t_h}^h] \mathbb{E}[S_{t_r}^r]}{\sqrt{\text{var}[S_{t_h}^h] \text{var}[S_{t_r}^r]}}, \quad (34)$$

is a symmetric function of the time horizons t_h and t_r , as one can easily verify starting from the definition of reversibility given in Section IV A. In contrast, the structure of its empirical estimation $\bar{\chi}(t_h, t_r)$ for the S&P500 time series shows some degrees of asymmetry. This is highlighted by the level curves plot in Fig. 9, also named “volatility mug shots” [18, 19]. Such an asymmetry is however rather mild and sample dependent, as illustrated by Figs. 9a and 9b where the whole S&P500 sample and the second half only are exploited, respectively. As far as our model is concerned, at variance with what pointed out in Ref. [25] for a different implementation of our ideas, we remark that such a mild time asymmetry is consistently reproduced. For instance, Fig. 9c displays the level curves of $\chi(t_h, t_r)$ corresponding to the complete model calibrated with $M = 42$.

In the various comparisons outlined in this Section we have used the average values defined by our calibrated model. In model-generated time series with a length of the order of that of the available S&P500 dataset, we have also inspected the fluctuations around these average values. In general, we have observed fluctuations that are consistent with those associated to the sample-dependence of the S&P500 time series.

VII. LONG-MEMORY AND SHORT-MEMORY VOLATILITY

An interesting feature for a model of asset evolution is the possibility of distinguishing between long-memory and short-memory contributions to the volatility. Since part of the short-memory random effects may be attributed to the impact of external information on the asset’s time evolution, such a distinction is also related to attempts in separating the endogenous and exogenous contributions to the volatility [64–70]. Indeed, although this should not be regarded as a clear cut distinction, one may reasonably expect that long-memory contributions could be ascribed to cooperative influences among the agents, whereas random volatility switches may also come from news reaching the market. In our model, albeit intimately combined together, the long-memory and short-memory components play their own distinct role in reproducing realistic financial features. The question then naturally arises about the possibility of identifying these two different contributions. For this reason, we propose here a procedure to localize the time restarts in a given finite realization $\{\bar{x}_t\}_{t=1}^T$ of a process which is assumed to be well represented by our model. Once the restarts are supposed to be known, we can identify the auto-regressive trajectory $\{\bar{y}_t\}_{t=1}^T$, thus succeeding in distinguishing between the two contributions.

To the purpose of locating restarts, we consider the probability of having a restart at a certain time t conditioned to the information available in a narrow time window centered in t with half-width τ . Namely,

$$\mathbb{P}[I_t = 1 | X_n = \bar{x}_n, |n - t| \leq \tau]. \quad (35)$$

The time restarts can thus be tentatively associated to the peaks of this probability. Since *a priori* we expect about νT time restarts, T being the length of the considered time series, we associated them to the highest νT peaks. In Fig. 10 $\tau = 2$ is used with respect to a model-generated time series. Conditioning the time restarts identification to more time series values by taking a larger value of τ would in principle provide better results. In practice however computational limitations force us to focus on small values of τ . Despite this restriction, in Fig. 10 we have been able to identify exactly 60% of the true restarts and about 70% with an uncertainty of two days. Fig. 11 displays the result of the same “time restarts analysis” applied to the S&P500 dataset.

Once the time restarts have been unveiled and the auto-regressive trajectory $\{\bar{y}_t\}_{t=1}^T$ thus identified, we can analyze the long-memory part of the volatility. Within our model, a convenient way of defining the long-memory volatility on the time horizon t is through the random variable

$$S_t \equiv \sqrt{\frac{1}{t} \sum_{n=1}^t Y_n^2}. \quad (36)$$

The PDF k_t of this variable is easily obtained when $t \leq M + 1$, due to the fact that f_t^Y reduces to a mixture of factorized Gaussian densities with the same variance. It turns out to be

$$k_t(s) = \int_0^\infty d\sigma \rho(\sigma) \frac{2^{1-\frac{t}{2}} s^{t-1} t^{\frac{t}{2}}}{\Gamma(\frac{t}{2}) \sigma^t} e^{-\frac{ts^2}{2\sigma^2}}. \quad (37)$$

In particular, if the function ρ is chosen according to Eq. (20), then k_t is explicitly found as

$$k_t(s) = \frac{2\beta^\alpha s^{t-1} t^{\frac{t}{2}}}{B\left(\frac{\alpha}{2}, \frac{t}{2}\right) (\beta^2 + s^2 t)^{\frac{\alpha+t}{2}}}, \quad (38)$$

where B is the Euler’s Beta function. On the empirical side, the distribution k_t can be sampled from the estimated auto-regressive path $\{\bar{y}_t\}_{t=1}^T$. Fig. 12 shows a comparison between theoretical and empirically detected long-memory component of the volatility distributions for model-generated time series with $t = M = 63$. Notice that as the model’s time series length T increases, the outcome of the present procedure becomes very close to the theoretical prediction in Eq. (38). This is particularly evident if, in place of using the restarts obtained through Eq. (35), we randomly choose them along the time series. Finally, the consistency of the S&P500 histogram with the theoretical prediction for k_M (Fig. 13) points out that our procedure for identifying the long-memory component of the volatility could be successfully applied to the real market evolution, having sufficiently long historical time series at disposal.

A distinction between long-memory and short-memory components of the volatility is not a standard practice in finance. However, we think that its consideration could open interesting perspectives in fields like risk evaluation and market regulation.

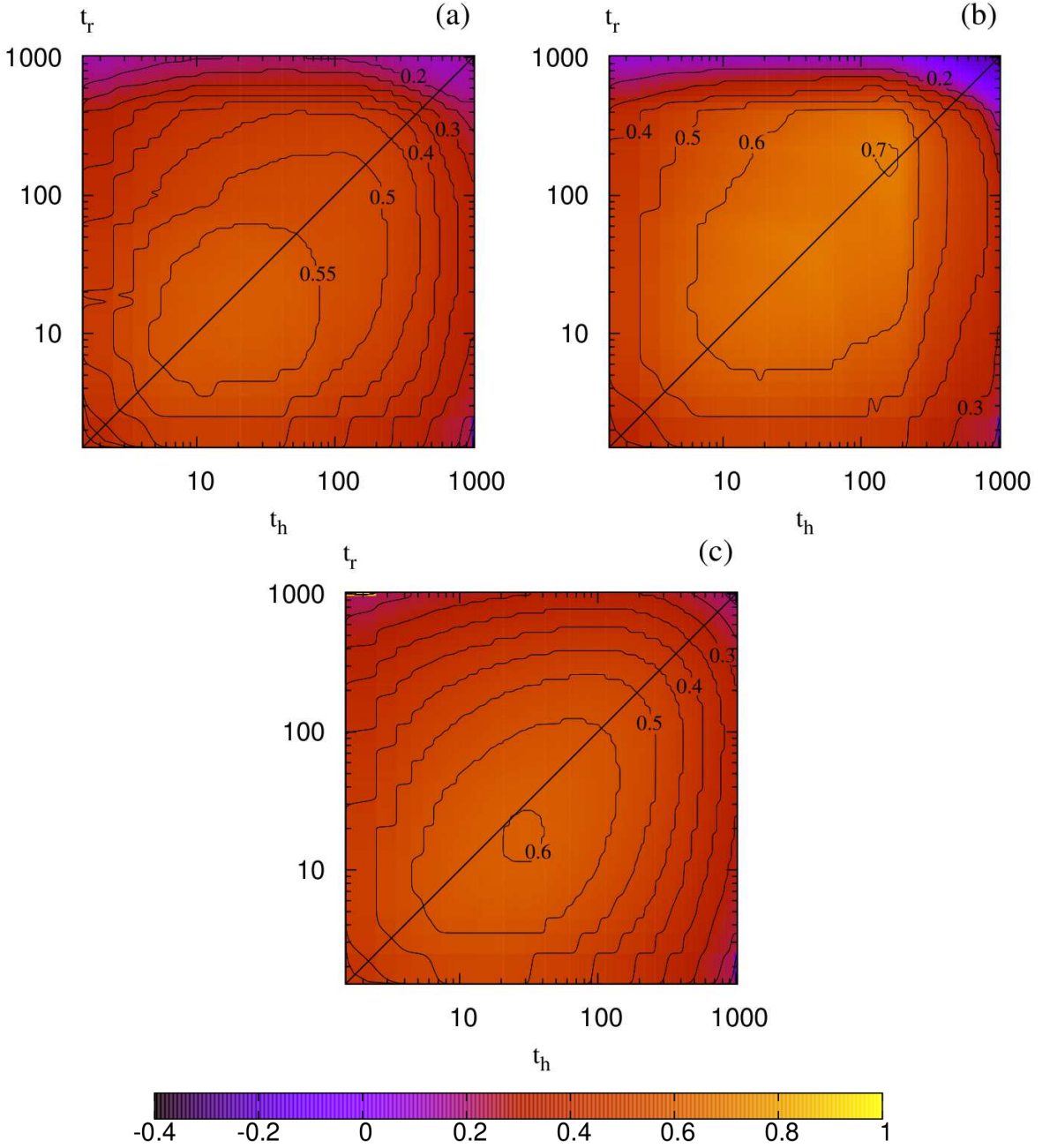


FIG. 9: Level curves plot of $\bar{\chi}(t_h, t_r)$, or volatility mug shots. (a) whole S&P500 time series ($T = 15385$); (b) second half of S&P500 time series ($T = 7694$); (c) model's prediction with the $M = 42$ -calibration.

VIII. IMPROVEMENTS AND FURTHER DEVELOPMENTS

Even if the present version of our model represents a significant advancement in terms of stylized-facts-reproduction-to-analytical-control ratio, some important empirical features like the leverage effect and the skewness of the return distribution are missing. Here we briefly discuss how both these effects can be reproduced by suitable improvements of the model.

The leverage effect refers to the presence in historical time series of a negative odd-even correlation of the kind $\mathbb{E}[X_1 X_t^2] < 0$. The model we have presented gives $\mathbb{E}[X_1 X_t^2] = 0$ for any t and, also, a symmetric returns distribution. So far, in favor of an initial simplicity we have kept the long-memory and short-memory components independent. The introduction of a dependence between these two processes, such as that arising when the latter is assumed somehow affected by the past values of the former (similarly, e.g., to the ideas outlined in Ref. [39]) could produce non-zero sign-volatility correlations

Model's time series

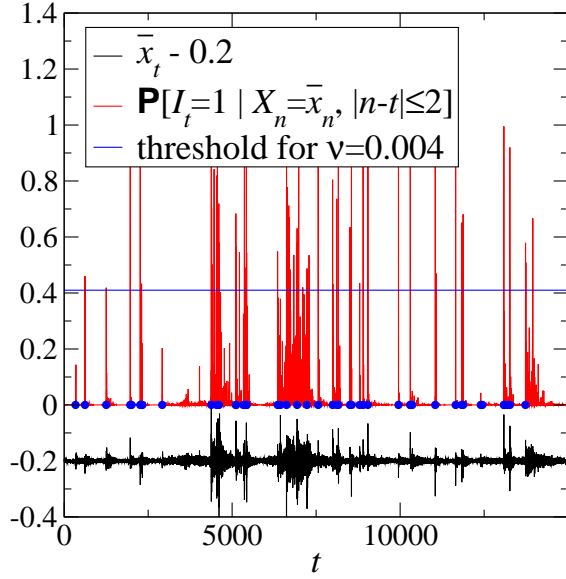


FIG. 10: A procedure to locate the restart. In black is depicted a $T = 12000$ -long time series generated by our model with the parameters $(\bar{D}, \bar{\nu}, \bar{\alpha}, \bar{\beta}) = (0.16, 0.004, 5.5, 0.14)$, associated to the $M = 63$ calibration. For convenience of inspection, the time series is vertically shifted by -0.2 . In red $\mathbb{P}[I_t = 1 | X_n = \bar{x}_n, |n - t| \leq 2]$ is reported. The blue line corresponds to the threshold for which νT restarts are detected; blue circles mark the true restarts generated by the dynamics.

$k_M(s)$

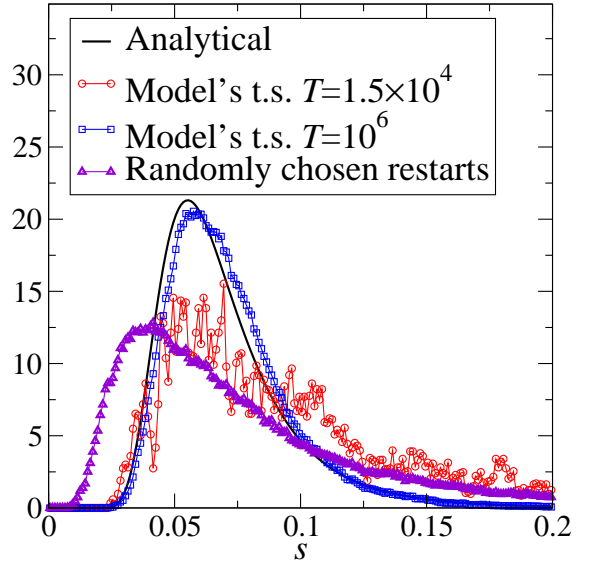


FIG. 12: Distribution of the long-memory component of the volatility: the continuous line is the theoretical prediction, Eq. (38); circles and squares refer to two time series of T data generated by the model with the $M = 63$ calibration parameter set; triangles are obtained from the time series with $T = 10^6$, with the time restarts chosen randomly.

S&P500

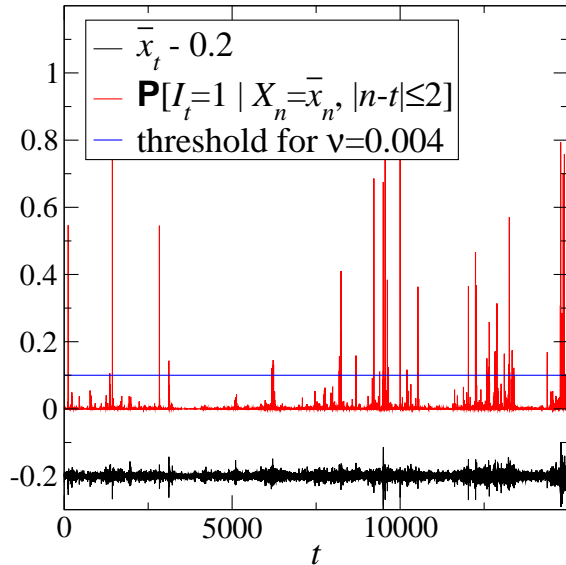


FIG. 11: Same as Fig. 10, but applied to the S&P500 historical time series. Here, of course, blue circles are absent.

$k_M(s)$

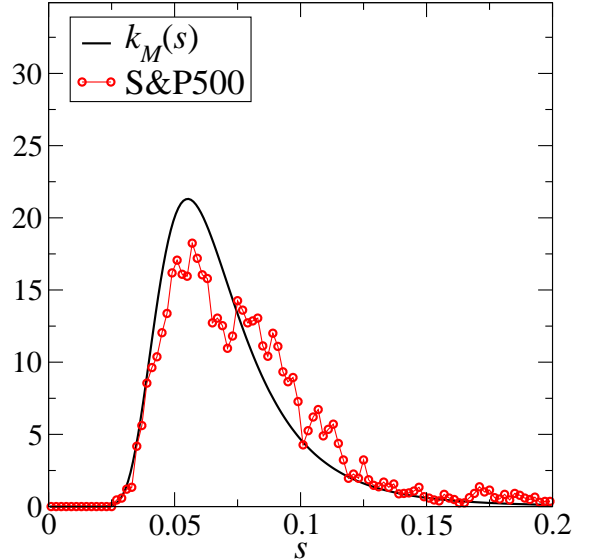


FIG. 13: Distribution of the long-memory component of the volatility for the S&P500 dataset (circles), compared with the model-based prediction, Eq. (38), (full line).

like the leverage effect. An appealing and potentially interesting way of doing this within our mathematical construction may simply consist in making time restarts dependent on the sign of the auto-regressive endogenous component. We sketch some arguments about this perspective.

Introducing the process $\{B_t\}_{t=1}^{\infty}$ of the signs of $\{Y_t\}_{t=1}^{\infty}$, defined as $B_t = 1$ if $Y_t \geq 0$ and $B_t = -1$ if $Y_t < 0$, in the Supplementary Material [40] we show that $\{B_t\}_{t=1}^{\infty}$ and the sequence $\{|Y_t|\}_{t=1}^{\infty}$ of the magnitude of Y_t 's are mutually independent for the model considered so far. Moreover $\{B_t\}_{t=1}^{\infty}$ results in a sequence of i.i.d. binary variables with $\mathbb{P}[B_1 = 1] = 1/2$, telling us that we have been tossing a fair coin to decide the sign of returns. These considerations allow one to recast our model as $X_t = a_{I_t} B_t |Y_t|$ with $\{I_t\}_{t=1}^{\infty}$, $\{B_t\}_{t=1}^{\infty}$, and $\{Y_t\}_{t=1}^{\infty}$ independent from each other.

In order to improve the model, we could then think in general at different alternatives. We could assume that the B_t 's take value different from -1 and $+1$ as, e.g., in Ref. [17]. Also, we could draw B_{t+1} independently of the past events, but making the restart occurrence $I_{t+1} = 1$ dependent on the value of B_t . In such a case, the process $\{(I_t, B_t)\}_{t=1}^{\infty}$ would result in a bivariate Markov chain, still independent of $\{Y_t\}_{t=1}^{\infty}$. We already know that a simple setting of this kind guarantees the martingale character, the stationarity, and the mixing properties of the returns' process $\{X_t\}_{t=1}^{\infty}$ defined as $X_t \equiv a_{I_t} B_t |Y_t|$. At the same time, a skewness in the return distribution is recovered by properly choosing the values assumed by the B_t 's. The leverage effect occurs then making negative returns more likely followed by a time restart than positive ones. Work is in progress along these lines.

Coming back to the model discussed in the present Paper, an interesting applicative perspective is the fact that its analytical handiness permits the derivation of closed-formulas for derivative pricing and the associated hedging strategy. As pointed out in [25], in the presence of a Gaussian mixture process for the underlying asset an obvious way of obtaining an arbitrage-free option price is by taking the average Black-Scholes price [7, 33, 62] according to the variance measure of the mixture. In the present approach, such a basic idea must be shaped in order to take into account two basic facts. In first place, the auto-regressive endogenous component implies that an effective variance measure of the Gaussian mixture is conditioned by the previous endogenous values of the process. On the other side, the Markov-switching process strongly influences the volatility. Thus, an effective way of identifying time restarts according to the scheme discussed in Section VII must be developed. In a related work in progress [38] we have been able to successfully tackle these two aspects and to produce an equivalent martingale measure which allows one to derive European option prices [33] in a closed form and to associate a natural hedging strategy with the underlying asset dynamics.

IX. CONCLUSIONS

Scaling and long range dependence have played a major role in the recent development of stochastic models of financial assets dynamics. This development proceeded parallel to the progressive realization that indeed scaling and multiscaling properties are themselves relevant stylized facts. A key achievement has been the multifractal model of asset returns (MMAR) proposed by Mandelbrot and coworkers [14]. This model introduced important features, like the possibility of multiscaling return distributions with finite variance and the long range dependence in the volatility, with uncorrelated returns. This long range dependence had been previously a peculiarity of ARCH or GARCH type models [3, 30–32], widely used in empirical finance. The difficulties mainly arising from the strict time reversal invariance of the MMAR has been overcome by subsequent proposals of multi-time-scale models [19, 20] which are somehow intermediate between GARCH processes and descriptions based on multiplicative cascades. However, a limitation of all the approaches mentioned above is due to the scarce analytical tractability and the difficulty in efficiently expressing the conditioning effect of past histories when applying them to VaR estimates or option pricing.

The model we presented here addresses the problem first posed by Bachelier over a century ago [63] and opens some interesting perspectives. From a methodological point of view, due to the roots in renormalization theory, it offers an example where scaling becomes a guiding criterion for the construction of a meaningful dynamics. This direction appears quite natural if we look at the development of complex systems theory in statistical physics. Scaling is normally regarded as a tool for unconditioned forecasting. Thanks to our renormalization group philosophy, here we have shown that scaling can also be exploited in order to obtain conditioned forecasting, which is of major importance in finance. This conditioned forecasting potential is based on the multivariate price return distributions like Eqs. (4) and (24), which one can construct on the basis of scaling properties.

The coexistence of exogenous and endogenous effects driving the dynamics of the markets has been recognized since long. Indeed, the variations of the assets' price and volatility cannot be explained only on the basis of arrival of new information on the market. A remarkable feature of our model is the fact that it embodies a natural and sound distinction between the long-memory endogenous influences and the short memory, partially exogenous ones on the volatility. Even if the distinction is model-based, the comparison with the S&P500 dataset has shown consistency with historical data.

In the relatively simple form discussed in this Paper, our model has important requisites for opening the way to useful applications. One of these applications, namely a closed-form formulation for pricing derivative assets, is presently under development [38]. Indeed, in view of the capability to account for a considerable number of styl-

ized facts, our model maintains a high degree of mathematical tractability. This tractability allows to rigorously derive important mathematical properties of the process and to set up successful calibration procedures.

A deep connection of our approach with ARCH models [3, 30–32] is the fact that we identify an auto-regressive scheme as a natural one on which to base the ergodic and stationary dynamics of our endogenous process. Remarkably, we are naturally led to this choice following our criteria based on scaling and on the quest for ergodicity and stationarity.

Our modeling is not based on a “microscopic”, agent based description [27–29], which should be regarded as a most fundamental and advanced stage at which to test the potential of statistical physics methods in finance. However, we believe that our results open in the field

novel perspectives thanks to the application of one of the most powerful methods available so far for the study of complexity in physics, the renormalization group approach. This approach provides an original, valuable insight into the statistical texture of return fluctuations, which is a key requisite for successful stochastic modeling.

Acknowledgments

We would like to thank J.-P. Bouchaud and M. Caporin for useful discussions. This work is supported by “Fondazione Cassa di Risparmio di Padova e Rovigo” within the 2008-2009 “Progetti di Eccellenza” program.

-
- [1] H. Kantz, and T. Schreiber, *Nonlinear Time Series Analysis*, 2nd edn. (Cambridge University Press 2004).
- [2] R. Shcherbakov, G. Yakovlev, D.L. Turcotte, and J.B. Rundle, *A model for the distribution of aftershock waiting times*, Phys. Rev. Lett. **95**, 218501 (2005).
- [3] D.J. Wilkinson, *Stochastic modelling for quantitative description of heterogeneous biological systems*, Nature Reviews Genetics **10**, 122 (2009).
- [4] P.Ch. Ivanov L.A. Nunes Amaral, A.L. Goldberger, S. Havlin, M.G. Rosenblum, Z.R. Struzik, and H.E. Stanley, *Multifractality in human heartbeat dynamics* Nature **399**, 461 (1999).
- [5] A.M. Petersen, J. Tenenbaum, S. Havlin, and H.E. Stanley, *Statistical Laws Governing Fluctuations in Word Use from Word Birth to Word Death*, Scientific Reports **2**, 313 (2012).
- [6] T. Preis, D.Y. Kenett, H.E. Stanley, D. Helbing, and E. Ben-Jacob, *Quantifying the Behavior of Stock Correlations Under Market Stress*, Scientific Reports **2**, 752 (2012).
- [7] J.-P. Bouchaud, and M. Potters, *Theory of Financial Risk and Derivative Pricing: from Statistical Physics to Risk Management*, 2nd edn. (Cambridge University Press, 2003).
- [8] R.S. Tsay, *Analysis of Financial Time Series* (John Wiley & Sons, 2002).
- [9] M. Musiela, and M. Rutkowski, *Martingale Methods in Financial Modelling*, 2nd edn. (Springer Verlag, 2005).
- [10] R. Cont, *Empirical properties of asset returns: stylized facts and statistical issues*, Quant. Fin. **1**, 223 (2001).
- [11] R. Cont, *Long range dependence in financial time series*, in E. Lutton, J. Levy Véhel eds. *Fractals in Engineering* (Springer-Verlag, New York, 2005).
- [12] J. Voigt, *The Statistical Mechanics of Financial Markets* (Springer, Berlin, 2001).
- [13] S. Ghashghaie, W. Breymann, J. Peinke, P. Talkner, Y. Dodge, *Turbulent cascades in foreign exchange markets*, Nature **381**, 767 (1996)
- [14] B. Mandelbrot, A. Fisher, and L. Calvet, *A Multifractal Model of Asset Returns* (Cowles Foundation Discussion Papers 1164, Cowles Foundation, Yale University, 1997)
- [15] J.C. Vassilicos, A. Demos, and F. Tata, *No evidence of chaos but some evidence of multifractals in the foreign exchange and the stock market* in A.J. Crilly, R.A. Earnshaw, H. Jones, eds. *Applications of Fractals and Chaos* (Springer, Berlin, 1993).
- [16] E. Bacry, J. Delour, and J.F. Muzy, *Modelling financial time series using multifractal random walks*, Physica A **299**, 84 (2001).
- [17] Z. Eisler, and J. Kertész, *Multifractal model of asset returns with leverage effect*, Physica A **343**, 603 (2004).
- [18] L. Borland, J.-P. Bouchaud, J.F. Muzy, and G.O. Zumbach, *The Dynamics of Financial Markets – Mandelbrot’s Multifractal Cascades, and beyond*, Science & Finance (CFM) working paper archive 500061, Science & Finance, Capital Fund Management, (2005).
- [19] G.O. Zumbach, M.M. Dacorogna, J.L. Olsen, and R.B. Olsen, *Measuring shock in financial markets*, Int. J. Theor. Appl. Finance **3**, 347 (2000).
- [20] L. Borland, and J.-P. Bouchaud, *On a Multi-Timescale Statistical Feedback Model for Volatility Fluctuations*, Science & Finance (CFM) working paper archive 500059, Science & Finance, Capital Fund Management (2005).
- [21] R.N. Mantegna, and H.E. Stanley, *Scaling behaviour in the dynamics of an economic index*, Nature **376**, 46 (1995); Nature **383**, 587 (1996).
- [22] R.N. Mantegna, H.E. Stanley, H. E., *An Introduction to Econophysics* (Cambridge University Press, Cambridge, UK, 2000).
- [23] F. Baldovin, and A.L. Stella, *Scaling and efficiency determine the irreversible evolution of a market*, Proc. Natl. Acad. Sci. USA **104**, 19741 (2007).
- [24] A.L. Stella, and F. Baldovin, *Anomalous scaling due to correlations: limit theorems and self-similar processes*, J. Stat. Mech. P02018 (2010).
- [25] P.P. Peirano, and D. Challet, *Baldovin-Stella stochastic volatility process and Wiener process mixtures*, Eur. Phys. J. B **85**, 276 (2012).
- [26] A. Andreoli, F. Caravenna, P. Dai Pra, and G. Posta, *Scaling and multiscaling in financial series: a simple model*, Adv. in Appl. Probab. **44**, 1018 (2012).
- [27] T. Lux, and M. Marchesi, *Scaling and criticality in a stochastic multi-agent model of a financial market*, Nature **397**, 498 (1999).

- [28] B. LeBaron, *Short-memory traders and their impact on group learning in financial markets*, Proc. Natl. Acad. Sci. USA **99**, 7201 (2002).
- [29] N. Alfi, M. Cristelli, L. Pietronero, and A. Zaccaria, *Minimal agent based model for financial markets I and II*, Europ. Phys. J. B **67**, 385 (2009).
- [30] R. Engle, *Estimates of the variances of U.S. inflation based upon the ARCH model*, Journal of Money, Credit and Banking **15**, 286 (1983).
- [31] T. Bollerslev, *Generalized autoregressive conditional heteroskedasticity*, Journal of Econometrics **31**, 307 (1986).
- [32] T. Bollerslev, R.F. Engle, and D.B. Nelson, *ARCH Models*, in Handbook of Econometrics, edited by R.F. Engle, D.L. McFadden (Elsevier, 1994), pp. 29593038.
- [33] J.C. Hull, *Options, Futures and Other Derivatives* (Prentice-Hall, 2000).
- [34] F. Baldovin, and A.L. Stella, *Central limit theorem for anomalous scaling due to correlations*, Phys. Rev. E **75**, 020101(R) (2007).
- [35] F. Baldovin, D. Bovina, F. Camana, and A.L. Stella, *Modeling the Non-Markovian, Non-stationary Scaling Dynamics of Financial Markets*, in F. Abergel, B. K. Chakrabarti, A. Chakraborti, and M. Mitra (eds.) *Econophysics of order-driven markets* (1st edn), (New Economic Windows, Springer 2011) pp. 239–252.
- [36] F. Baldovin, F. Camana, M. Caporin, and A. L. Stella, *Ensemble properties of high frequency data and intraday trading rules*, to be published (2013) [arXiv:1202.2447].
- [37] F. Baldovin, F. Camana, M. Caraglio, A.L. Stella, and M. Zamparo *Aftershock prediction for high-frequency financial markets' dynamics* in F. Abergel, B.K. Chakrabarti, A. Chakraborti, A. Ghosh, eds., *Econophysics of Systemic Risk and Network Dynamics* (New Economic Windows, Springer 2013), pp 49-58.
- [38] F. Baldovin, M. Caporin, M. Caraglio, A.L. Stella, and M. Zamparo, *Option pricing with anomalous scaling and switching volatility*, to be published (2013) [arXiv:1307.6322].
- [39] J.-P. Bouchaud, A. Matacz, and M. Potters, *Leverage Effect in Financial Markets: The Retarded Volatility Model* Phys. Rev. Lett. **87**, 228701 (2001).
- [40] M. Zamparo, F. Baldovin, M. Caraglio, and A.L. Stella, *Scaling symmetry, renormalization, and time series modeling – Supplementary Material*, (2013).
- [41] B.B. Mandelbrot, and J.W. Van Ness, *Fractional Brownian motions, fractional noises and applications*, SIAM Review **10**, 422 (1968).
- [42] R.T. Baillie, T. Bollerslev, and H.O. Mikkelsen, *Fractionally integrated generalized autoregressive conditional heteroskedasticity*, Journal of Econometrics **74**, 3 (1996).
- [43] L.P. Kadanoff, *Statistical Physics, Statics, Dynamics and Renormalization*, (World Scientific, Singapore 2005).
- [44] G. Jona-Lasinio, *Renormalization group and probability theory*, Phys. Rep. **352**, 439 (2001).
- [45] N. Goldenfeld, *Lectures on phase transitions and the renormalization group*, (Addison-Wesley, 1993).
- [46] U. Frisch, *Turbulence: The Legacy of A.N. Kolmogorov* (Cambridge University Press, Cambridge, 1995).
- [47] T. Di Matteo, *Multi-scaling in finance*, Quant. Fin. **7**, 21 (2007).
- [48] M. Zamparo, F. Baldovin, M. Caraglio, and A.L. Stella, in preparation (2013).
- [49] I.J. Schoenberg, *Metric Spaces and Completely Monotone Functions*, Ann. Math. **39**, 811 (1938).
- [50] D.J. Aldous, *Exchangeability and related topics*, Lecture Notes in Mathematics **1117**, 1 (1985).
- [51] G. Iori *Scaling and Multiscaling in Financial Markets*, in *Disordered and Complex Systems*, ed. P. Sollich et al., AIP Conference Proceedings **553**, 297 (2001).
- [52] T. Di Matteo, T. Aste, and M.M. Dacorogna, *Long-term memories of developed and emerging markets: Using the scaling analysis to characterize their stage of development*, J. Bank. & Fin. **29**, 827 (2005).
- [53] A. Gerig, J. Vicente, and M.A. Fuentes, *Model for non-Gaussian intraday stock returns* Phys. Rev. E **80**, 065102R (2009).
- [54] S. Miccichè, G. Bonanno, F. Lillo, and R.N. Mantegna, *Volatility in financial markets: stochastic models and empirical results*, Physica A **314**, 756 (2002).
- [55] J.D. Hamilton and R. Susmel, *Autoregressive Conditional Heteroskedasticity and Changes in Regime*, Journal of Econometrics **64**, 307 (1994).
- [56] E.F. Fama, *Efficient capital markets: review of theory and empirical work*, Journal of Finance **25**, 383-417 (1970).
- [57] E.F. Fama, *Efficient capital markets: II*, J. Finance **46**, 1575 (1991).
- [58] R.T. Baillie, *Long memory processes and fractional integration in econometrics*, Journal of Econometrics **73**, 5-59 (1996).
- [59] A.R. Hall, *Generalized Method of Moments (Advanced Texts in Econometrics)* (Oxford University Press, 2005).
- [60] G. Zumbach, *Time reversal invariance in finance* Quant. Fin. **9**, 505 (2009).
- [61] P.E. Lynch, and G.O. Zumbach, *Market heterogeneities and the causal structure of volatility* Quant. Fin. **3**, 320 (2003).
- [62] F. Black, and M. Scholes, *The Pricing of Options and Corporate Liabilities*, J. Polit. Econ. **81**, 637 (1973).
- [63] L. Bachelier, *Theorie de la speculation*, Ann. Sci. Ecole Norm. Sup. **17**, 21 (1900).
- [64] S.J. Hardiman, N. Bercot, and J.-P. Bouchaud, *Critical reflexivity in financial markets: a Hawkes process analysis*, [arXiv:1302.1405v2].
- [65] A. Joulin, A. Lefevre, D. Grunberg, and J.-P. Bouchaud *Stock price jumps: news and volume play a minor role*, Wilmott Magazine (September-October, 2008) 1.
- [66] D.M. Cutler, J.M. Poterba, D. Grunberg, and L.H. Summers, *What moves stock prices*, Journal of Portfolio Management **15** no. 3, 555 (1989).
- [67] V. Filimonov, and D. Sornette, *Quantifying reflexivity in financial markets: towards a prediction of flash crashes*, Phys. Rev. E **85**, 056108 (2012).
- [68] V. Filimonov, S. Wheatley, and D. Sornette, *Effective Measure of Endogeneity for the Autoregressive Conditional Duration Point Processes via Mapping to the Self-Excited Hawkes Process*, [arXiv:1306.2245].
- [69] D. Sornette, *Endogenous versus Exogenous Origins of Crises*, Extreme events in nature and society, Springer (2006).
- [70] D. Sornette, F. Deschâtres, T. Gilbert, and Y. Ageon, *Endogenous versus exogenous shocks in complex networks: An empirical test using book sale rankings*, Phys. Rev. Lett. **93**, 228701 (2004).
- [71] This version of the model results to be the discrete-time counterpart of the one considered in Ref. [26] after one keeps a constant average volatility.

Scaling symmetry, renormalization, and time series modeling Supplementary Material

Marco Zamparo

*Dipartimento di Fisica, Sezione INFN, CNISM, and Università di Padova, Via Marzolo 8, I-35131 Padova, Italy and
HuGeF, Via Nizza 52, 10126 Torino, Italy*

Fulvio Baldovin, Michele Caraglio, and Attilio L. Stella

Dipartimento di Fisica, Sezione INFN, CNISM, and Università di Padova, Via Marzolo 8, I-35131 Padova, Italy

I. INTRODUCTION

This Supplementary Material provides proofs of the model properties announced in the Main Text. In Section II the joint PDF's of the process $\{X_t\}_{t=1}^{\infty}$ are derived from the definition of the long-memory and short-memory components $\{Y_t\}_{t=1}^{\infty}$ and $\{I_t\}_{t=1}^{\infty}$, respectively. Section III is devoted to prove the stationarity of $\{X_t\}_{t=1}^{\infty}$, while in Section IV we show that $\{Y_t\}_{t=1}^{\infty}$ is a reversible sequence and that the series of its sign is independent of $\{|Y_t|\}_{t=1}^{\infty}$. In Sections V and VI we reconsider the issue of the tail of the single-variable PDF f_1^X and the scaling features of our model supplying a more complete study. In Section VI we prove some properties of what we called the “null” and the “complete” models in the Main Text, in particular showing that the endogenous component $\{Y_t\}_{t=1}^{\infty}$ of the complete model [with the choice in Eq. (20) of the Main Text for the function ρ] is an ARCH process. Lastly, Section VIII contains a detailed analysis of the autocorrelation r_q^X .

II. PDF'S ASSOCIATED WITH THE MODEL

Here we derive the joint PDF's of the increments $\{X_t\}_{t=1}^{\infty}$, reported in Eq. (23) in the Main Text. The derivation exploits the features of the hidden processes $\{Y_t\}_{t=1}^{\infty}$ and $\{I_t\}_{t=1}^{\infty}$. To this and further purposes, we shall work with the expectation values of test functions. Unless explicitly stated, we will implicitly assume that such expectation values exist.

Given $t \geq 1$ and a test function F on \mathbb{R}^t , we have

$$\begin{aligned} \mathbb{E}[F(X_1, \dots, X_t)] &= \mathbb{E}[F(a_{I_1} Y_1, \dots, a_{I_t} Y_t)] \\ &= \sum_{i_1=1}^{\infty} \cdots \sum_{i_t=1}^{\infty} \mathbb{E}[F(a_{i_1} Y_1, \dots, a_{i_t} Y_t) \delta_{I_1 i_1} \cdots \delta_{I_t i_t}], \end{aligned} \quad (1)$$

where as usual δ denotes Kronecker's symbol. On the other hand, recalling that $\{Y_t\}_{t=1}^{\infty}$ and $\{I_t\}_{t=1}^{\infty}$ are mutually independent, the following factorization holds:

$$\begin{aligned} \mathbb{E}[F(a_{i_1} Y_1, \dots, a_{i_t} Y_t) \delta_{I_1 i_1} \cdots \delta_{I_t i_t}] &= \mathbb{E}[F(a_{i_1} Y_1, \dots, a_{i_t} Y_t)] \cdot \mathbb{E}[\delta_{I_1 i_1} \cdots \delta_{I_t i_t}] \\ &= \mathbb{E}[F(a_{i_1} Y_1, \dots, a_{i_t} Y_t)] \cdot \mathbb{P}[I_1 = i_1, \dots, I_t = i_t]. \end{aligned} \quad (2)$$

Thus, plugging this in Eq. (1), we obtain the chain of identities

$$\begin{aligned} \mathbb{E}[F(X_1, \dots, X_t)] &= \sum_{i_1=1}^{\infty} \cdots \sum_{i_t=1}^{\infty} \mathbb{E}[F(a_{i_1} Y_1, \dots, a_{i_t} Y_t)] \cdot \mathbb{P}[I_1 = i_1, \dots, I_t = i_t] \\ &= \sum_{i_1=1}^{\infty} \cdots \sum_{i_t=1}^{\infty} \mathbb{P}[I_1 = i_1, \dots, I_t = i_t] \cdot \\ &\quad \cdot \int_{\mathbb{R}} dy_1 \cdots \int_{\mathbb{R}} dy_t F(a_{i_1} y_1, \dots, a_{i_t} y_t) f_t^Y(y_1, \dots, y_t) \\ &= \int_{\mathbb{R}} dx_1 \cdots \int_{\mathbb{R}} dx_t F(x_1, \dots, x_t) \cdot \\ &\quad \cdot \sum_{i_1=1}^{\infty} \cdots \sum_{i_t=1}^{\infty} \mathbb{P}[I_1 = i_1, \dots, I_t = i_t] \frac{f_t^Y(x_1/a_{i_1}, \dots, x_t/a_{i_t})}{a_{i_1} \cdots a_{i_t}}. \end{aligned} \quad (3)$$

The last equality is the consequence of a simple change of variables in the integrals. This result, combined with the arbitrariness of F , clearly shows that the joint probability density distribution of (X_1, \dots, X_t) is

$$\begin{aligned} f_t^X(x_1, \dots, x_t) &\equiv \sum_{i_1=1}^{\infty} \cdots \sum_{i_t=1}^{\infty} \mathbb{P}[I_1 = i_1, \dots, I_t = i_t] \frac{f_t^Y(x_1/a_{i_1}, \dots, x_t/a_{i_t})}{a_{i_1} \cdots a_{i_t}} \\ &= \sum_{i_1=1}^{\infty} \cdots \sum_{i_t=1}^{\infty} W(i_t, i_{t-1}) \cdots W(i_2, i_1) \pi(i_1) \frac{f_t^Y(x_1/a_{i_1}, \dots, x_t/a_{i_t})}{a_{i_1} \cdots a_{i_t}}. \end{aligned} \quad (4)$$

As far as the density f_t^Y is concerned, let us recall that $f_t^Y = \varphi_t$ for $t \leq M+1$ where

$$\varphi_t(y_1, \dots, y_t) = \int_0^{\infty} d\sigma \rho(\sigma) \prod_{n=1}^t \mathcal{N}_{\sigma}(y_n). \quad (5)$$

Moreover, solving Eq. (14) of the Main Text, we explicitly get f_t^Y also when $t > M+1$ as

$$f_t^Y(y_1, \dots, y_t) = \frac{\prod_{n=1}^{t-M} \varphi_{M+1}(y_n, \dots, y_{n+M})}{\prod_{n=2}^{t-M} \varphi_M(y_n, \dots, y_{n+M-1})}. \quad (6)$$

III. STATIONARITY

This Section is devoted to prove the strict stationarity of the process $\{X_t\}_{t=1}^{\infty}$, for which we must verify that (X_n, \dots, X_{n+t-1}) is distributed as (X_1, \dots, X_t) for any $n \geq 1$ and $t \geq 1$. As a matter of fact, $\{X_t\}_{t=1}^{\infty}$ inherits this property from the hidden processes $\{Y_t\}_{t=1}^{\infty}$ and $\{I_t\}_{t=1}^{\infty}$ and so proving the strict stationarity of $\{Y_t\}_{t=1}^{\infty}$ and $\{I_t\}_{t=1}^{\infty}$ is the main issue. Let us assume for a moment that we know that (Y_n, \dots, Y_{n+t-1}) and (I_n, \dots, I_{n+t-1}) are distributed as (Y_1, \dots, Y_t) and (I_1, \dots, I_t) , respectively, for any $n \geq 1$ and $t \geq 1$. Then, given n, t , and a test function F on \mathbb{R}^t and exploiting again the independence between $\{Y_t\}_{t=1}^{\infty}$ and $\{I_t\}_{t=1}^{\infty}$, we obtain

$$\begin{aligned} \mathbb{E}[F(X_n, \dots, X_{n+t-1})] &= \mathbb{E}[F(a_{I_n} Y_n, \dots, a_{I_{n+t-1}} Y_{n+t-1})] \\ &= \sum_{i_1=1}^{\infty} \cdots \sum_{i_t=1}^{\infty} \mathbb{E}[F(a_{i_1} Y_n, \dots, a_{i_t} Y_{n+t-1})] \cdot \mathbb{P}[I_n = i_1, \dots, I_{n+t-1} = i_t] \\ &= \sum_{i_1=1}^{\infty} \cdots \sum_{i_t=1}^{\infty} \mathbb{E}[F(a_{i_1} Y_1, \dots, a_{i_t} Y_t)] \cdot \mathbb{P}[I_1 = i_1, \dots, I_t = i_t] \\ &= \mathbb{E}[F(X_1, \dots, X_t)], \end{aligned} \quad (7)$$

where the third equality is due to the hypothesis of stationarity of both $\{Y_t\}_{t=1}^{\infty}$ and $\{I_t\}_{t=1}^{\infty}$. The arbitrariness of F then tells us that (X_n, \dots, X_{n+t-1}) is distributed as (X_1, \dots, X_t) .

The stationarity of $\{I_t\}_{t=1}^{\infty}$ was already discussed in the Main Text and is the consequence of the fact that π is the invariant distribution of W . Thus, now we only have to analyze the process $\{Y_t\}_{t=1}^{\infty}$. In order to prove the strict stationarity of this process, let us observe that for any $n > M+1$, isolating the first terms in the products of Eq. (6), we get the identity

$$f_n^Y(y_1, \dots, y_n) = \frac{\varphi_{M+1}(y_1, \dots, y_{M+1})}{\varphi_M(y_2, \dots, y_{M+1})} f_{n-1}^Y(y_2, \dots, y_n). \quad (8)$$

Then, the fact that

$$\int_{\mathbb{R}} dy_1 \varphi_{M+1}(y_1, \dots, y_{M+1}) = \varphi_M(y_2, \dots, y_{M+1}) \quad (9)$$

leads us to the result

$$\int_{\mathbb{R}} dy_1 f_n^Y(y_1, \dots, y_n) = f_{n-1}^Y(y_2, \dots, y_n), \quad (10)$$

which is also valid for $n \leq M + 1$, where $f_n^Y = \varphi_n$, and hence for any n . This relation allows us to prove that

$$\mathbb{E}[F(Y_{n+1}, \dots, Y_{n+t})] = \mathbb{E}[F(Y_n, \dots, Y_{n+t-1})] \quad (11)$$

for any $n \geq 1$ and any function F on \mathbb{R}^t . Indeed

$$\begin{aligned} \mathbb{E}[F(Y_{n+1}, \dots, Y_{n+t})] &= \int_{\mathbb{R}} dy_1 \cdots \int_{\mathbb{R}} dy_{n+t} F(y_{n+1}, \dots, y_{n+t}) f_{n+t}^Y(y_1, \dots, y_{n+t}) \\ &= \int_{\mathbb{R}} dy_2 \cdots \int_{\mathbb{R}} dy_{n+t} F(y_{n+1}, \dots, y_{n+t}) f_{n+t-1}^Y(y_2, \dots, y_{n+t}) \\ &= \int_{\mathbb{R}} dy_1 \cdots \int_{\mathbb{R}} dy_{n+t-1} F(y_n, \dots, y_{n+t-1}) f_{n+t-1}^Y(y_1, \dots, y_{n+t-1}) \\ &= \mathbb{E}[F(Y_n, \dots, Y_{n+t-1})], \end{aligned} \quad (12)$$

where we have made use of Eq. (10) to obtain the second equality and we have just re-labeled the variables to get the third. The iteration of Eq. (11) then provides

$$\mathbb{E}[F(Y_n, \dots, Y_{n+t-1})] = \mathbb{E}[F(Y_1, \dots, Y_t)], \quad (13)$$

which states the stationarity of the process $\{Y_t\}_{t=1}^\infty$. \square

IV. REVERSIBILITY AND SIGN-MAGNITUDE INDEPENDENCE OF THE ENDOGENOUS COMPONENT

In the Main Text we pointed out that the process $\{Y_t\}_{t=1}^\infty$ is reversible, namely that $(Y_t, Y_{t-1}, \dots, Y_1)$ is distributed as $(Y_1, \dots, Y_{t-1}, Y_t)$ for any $t \geq 1$. Here we provide the proof verifying that

$$f_t^Y(y_t, y_{t-1}, \dots, y_1) = f_t^Y(y_1, \dots, y_{t-1}, y_t) \quad (14)$$

for any $t \geq 1$ and $(y_1, \dots, y_{t-1}, y_t) \in \mathbb{R}^t$. This identity descends from the invariance of φ_t with respect to permutations of its arguments and is evident if $t \leq M + 1$. At the same time, when $t > M + 1$, replacing $(y_1, \dots, y_{t-1}, y_t)$ with $(y_t, y_{t-1}, \dots, y_1)$ in Eq. (6) and rearranging the indexes, we obtain

$$\begin{aligned} f_t^Y(y_t, y_{t-1}, \dots, y_1) &= \frac{\prod_{n=1}^{t-M} \varphi_{M+1}(y_{t-n+1}, \dots, y_{t-n-M+1})}{\prod_{n=2}^{t-M} \varphi_M(y_{t-n+1}, \dots, y_{t-n-M+2})} \\ &= \frac{\prod_{n=1}^{t-M} \varphi_{M+1}(y_{n+M}, \dots, y_n)}{\prod_{n=2}^{t-M} \varphi_M(y_{n+M-1}, \dots, y_n)}. \end{aligned} \quad (15)$$

The exchangeability of the arguments of φ_{M+1} and φ_M , again, gives Eq. (14). \square

In Section VIII of the Main Text, in order to propose possible extensions of the model, we also mentioned that the sign and the magnitude of $\{Y_t\}_{t=1}^\infty$ constitute two independent processes, the former being a sequence of i.i.d. binary variables taking values in $\mathbb{Z}_2 \equiv \{-1, +1\}$ with equal probabilities. This fact follows from the symmetry of $f_t^Y(y_1, \dots, y_t)$ with respect to any of its arguments. Setting $B_t = \text{sgn}(Y_t)$ with $\text{sgn}(y) = 1$ if $y \geq 0$ and $\text{sgn}(y) = -1$ if $y < 0$, to prove the above two statements we have to check that for any $t \geq 1$ and any test functions F on \mathbb{Z}_2^t and G on \mathbb{R}^t the identity

$$\mathbb{E}[F(B_1, \dots, B_t) G(|Y_1|, \dots, |Y_t|)] = \mathbb{E}[F(B_1, \dots, B_t)] \cdot \mathbb{E}[G(|Y_1|, \dots, |Y_t|)] \quad (16)$$

and the relation

$$\mathbb{E}[F(B_1, \dots, B_t)] = 2^{-t} \sum_{b_1 \in \mathbb{Z}_2} \cdots \sum_{b_t \in \mathbb{Z}_2} F(b_1, \dots, b_t) \quad (17)$$

hold.

For a general F on \mathbb{R}^t we have the simple equality

$$\int_{\mathbb{R}} dy_1 \cdots \int_{\mathbb{R}} dy_t F(y_1, \dots, y_t) = \int_0^\infty dy_1 \cdots \int_0^\infty dy_t \sum_{b_1 \in \mathbb{Z}_2} \cdots \sum_{b_t \in \mathbb{Z}_2} F(b_1 y_1, \dots, b_t y_t). \quad (18)$$

Thus, we find that

$$\begin{aligned} \mathbb{E}[F(B_1, \dots, B_t) G(|Y_1|, \dots, |Y_t|)] &= \int_{\mathbb{R}} dy_1 \cdots \int_{\mathbb{R}} dy_t F(\text{sgn}(y_1), \dots, \text{sgn}(y_t)) G(|y_1|, \dots, |y_t|) f_t^Y(y_1, \dots, y_t) \\ &= \int_0^\infty dy_1 \cdots \int_0^\infty dy_t \sum_{b_1 \in \mathbb{Z}_2} \cdots \sum_{b_t \in \mathbb{Z}_2} F(b_1, \dots, b_t) G(y_1, \dots, y_t) f_t^Y(y_1, \dots, y_t) \\ &= 2^{-t} \sum_{b_1 \in \mathbb{Z}_2} \cdots \sum_{b_t \in \mathbb{Z}_2} F(b_1, \dots, b_t) \cdot \\ &\quad \cdot 2^t \int_0^\infty dy_1 \cdots \int_0^\infty dy_t G(y_1, \dots, y_t) f_t^Y(y_1, \dots, y_t) \\ &= 2^{-t} \sum_{b_1 \in \mathbb{Z}_2} \cdots \sum_{b_t \in \mathbb{Z}_2} F(b_1, \dots, b_t) \cdot \mathbb{E}[G(|Y_1|, \dots, |Y_t|)], \end{aligned} \quad (19)$$

where both the second and the last equalities are due to Eq. (18) and the symmetry of f_t^Y . Plugging here $G(y_1, \dots, y_t) = 1$ at first, we get Eq. (17). Eq. (16) is then a consequence of Eqs. (17) and (19). \square

V. TAIL BEHAVIOR OF f_1^X

In the Main Text we considered the issue about the tail of f_1^X very briefly. Here we provide a more extended discussion on this point studying the expectation $\mathbb{E}[|X_1|^q]$ for $q > 0$. In addition, we need to consider similar expectations also below in this Supplementary Material.

The independence between a_{I_1} and Y_1 allows us to write $\mathbb{E}[|X_1|^q] = \mathbb{E}[a_{I_1}^q] \mathbb{E}[|Y_1|^q]$. Since Eq. (19) of the Main Text for the sequence $\{a_i\}_{i=1}^\infty$ makes $\mathbb{E}[a_{I_1}^q]$ always finite, we realize that $\mathbb{E}[|X_1|^q]$ is finite if and only if $\mathbb{E}[|Y_1|^q]$ is finite. On the other hand, $\mathbb{E}[|Y_1|^q]$ is finite if and only if $\int_0^\infty \sigma^q \rho(\sigma) d\sigma$ is so. Indeed, from the definitions of f_1^Y and φ_1 [Eqs. (13) and (15) of the Main Text, respectively] we get

$$\begin{aligned} \mathbb{E}[|Y_1|^q] &= \int_{\mathbb{R}} |x|^q \mathcal{N}_1(x) \cdot \int_0^\infty \sigma^q \rho(\sigma) d\sigma \\ &= \frac{2^{\frac{q}{2}}}{\sqrt{\pi}} \Gamma\left(\frac{q+1}{2}\right) \int_0^\infty \sigma^q \rho(\sigma) d\sigma, \end{aligned} \quad (20)$$

where Γ is the Euler's Gamma function. Thus we discover that $\mathbb{E}[|X_1|^q]$ and $\mathbb{E}[|Y_1|^q]$, and the tails of f_1^X as a consequence, are only ruled by the last factor on the r.h.s. of Eq. (20), i.e. by ρ . In particular, if the function ρ decays according to a power law as $\sigma^{-\alpha-1}$ for large σ , then f_1^X inherits the same feature and displays fat tails with the same tail index α .

In the Main Text we also noticed that an effective fat tail scenario can be obtained also by considering suitable small values of the restart probability ν if $D < 1/2$. In order to shed light on this issue, we need to consider the limit of f_1^X when ν goes to zero. Nevertheless, such a limit is meaningless if we do not rescale the function ρ properly with ν since, if ρ is kept fixed in the limit procedure, then f_1^X concentrates around zero. The reason is that, when restarts get very rare, the random time $\{I_t\}_{t=1}^\infty$ tends to never go back to 1, reaching very large values in equilibrium conditions. As a consequence, when $D < 1/2$ the rescaling factor a_{I_1} tends to vanish and thus the mixture giving f_1^X becomes dominated by component distributions having a vanishing variance. If we want then to keep the variance of the random variable X_1 independent of ν , we must fix a function ρ' which does not depend on ν and define ρ according to

$$\rho(\sigma) \equiv \sqrt{\mathbb{E}[a_{I_1}^2]} \rho'\left(\sqrt{\mathbb{E}[a_{I_1}^2]} \sigma\right). \quad (21)$$

Indeed, Eq. (20) now provides

$$\mathbb{E}[|X_1|^q] = \mathbb{E}[a^q(I_1)]\mathbb{E}[|Y_1|^q] = \frac{2^{\frac{q}{2}}}{\sqrt{\pi}}\Gamma\left(\frac{q+1}{2}\right)\frac{\mathbb{E}[a^q(I_1)]}{\mathbb{E}[a^2(I_1)]^{\frac{q}{2}}}\int_0^\infty\sigma^q\rho'(\sigma)d\sigma, \quad (22)$$

which in particular entails

$$\mathbb{E}[X_1^2] = \int_0^\infty\sigma^2\rho'(\sigma)d\sigma. \quad (23)$$

In this framework the fluctuations of X_1 do not shrink in the limit $\nu \rightarrow 0$ and we obtain

$$\lim_{\nu \rightarrow 0^+}\mathbb{E}[|X_1|^q] = \frac{2^{\frac{q}{2}}}{\sqrt{\pi}}\frac{\Gamma(\frac{q+1}{2})\Gamma(\frac{2-(1-2D)q}{2})}{\Gamma^{\frac{q}{2}}(2D)}\int_0^\infty\sigma^q\rho'(\sigma)d\sigma \quad (24)$$

if $(1/2 - D)q < 1$ and $\lim_{\nu \rightarrow 0^+}\mathbb{E}[|X_1|^q] = \infty$ otherwise. We thus get the proof that fat tails with index $2/(1 - 2D)$ appear in this limit situation. It is clear that a function ρ' which endows the model with tails characterized by a tail index $\alpha < 2/(1 - 2D)$ hides this effect.

We conclude sketching the computation of this limit. To this purpose, it is convenient to introduce the notation of asymptotic equivalence: given two generic functions F and G of ν , we shall write $F \sim G$ to say that $\lim_{\nu \rightarrow 0^+} F(\nu)/G(\nu) = 1$. Then, if $\{\psi_i\}_{i=1}^\infty$ is a sequence for which there exists $\gamma > 0$ and $l > 0$ such that $\lim_{i \rightarrow \infty} i^\gamma \psi_i = l$, we have that as ν goes to zero

$$\mathbb{E}[\psi_{I_1}] = \sum_{i=1}^\infty \psi_i \nu (1-\nu)^{i-1} \sim \begin{cases} l\Gamma(1-\gamma)\nu^\gamma & \text{if } 0 < \gamma < 1; \\ l\nu|\ln\nu| & \text{if } \gamma = 1; \\ \nu \sum_{i=1}^\infty \psi_i & \text{if } \gamma > 1. \end{cases} \quad (25)$$

The last series is convergent. The instance $\gamma \leq 1$ is a consequence of the Karamata's theorem [1], whereas the case $\gamma > 1$ is due to the Abel's theorem [1]. The limit value of Eq. (22) follows then by noticing that $a_i = \sqrt{i^{2D} - (i-1)^{2D}}$ implies $\lim_{i \rightarrow \infty} i^{1/2-D} a_i = \sqrt{2D}$. \square

VI. SCALING FEATURES

We reconsider here the scaling features of our model at short time scales, providing a deeper insight into the properties outlined in Section IV B of the Main Text.

To begin with, we derive the distribution of the aggregated return $X_1 + \dots + X_t$ when $t \leq M + 1$. To this aim, let us observe that from Eqs. (4) and (5), thanks to the stability of Gaussian distributions with respect to linear combinations of independent Gaussian variables, we attain

$$\mathbb{E}[F(X_1 + \dots + X_t)] = \int_{\mathbb{R}} dx F(x) \mathbb{E}\left[\int_0^\infty d\sigma \rho(\sigma) \mathcal{N}_{\sqrt{a_{I_1}^2 + \dots + a_{I_t}^2}}\sigma(x)\right] \quad (26)$$

for any test function F on \mathbb{R} . This identity clearly shows that, if $t \leq M + 1$, the PDF of $X_1 + \dots + X_t$ is given as a function of x by the expression

$$\mathbb{E}\left[\int_0^\infty d\sigma \rho(\sigma) \mathcal{N}_{\sqrt{a_{I_1}^2 + \dots + a_{I_t}^2}}\sigma(x)\right]. \quad (27)$$

We notice that this PDF cannot be obtained by simply rescaling f_1^X , except if $\nu = 1$ or $a_i = 1$ for any i in which case the normal scaling behavior with exponent $1/2$ is recovered. Thus, in general the model accounts for a richer scenario than a perfect time-scale-invariance framework, as we know.

Choosing in Eq. (26) $F(x) = |x|^q$, with $q \geq 0$ such that $\int_0^\infty \sigma^q \rho(\sigma) d\sigma < \infty$, we get

$$\mathbb{E}[|X_1 + \dots + X_t|^q] = \frac{2^{\frac{q}{2}}}{\sqrt{\pi}}\Gamma\left(\frac{q+1}{2}\right)\int_0^\infty\sigma^q\rho(\sigma)d\sigma \cdot \mathbb{E}[(a_{I_1}^2 + \dots + a_{I_t}^2)^{\frac{q}{2}}]. \quad (28)$$

This result allows us to prove Eq. (27) of the Main Text:

$$m_q^X(t) = \frac{\mathbb{E}[|X_1 + \dots + X_t|^q]}{\mathbb{E}[|X_1|^q]} = \frac{\mathbb{E}[(a_{I_1}^2 + \dots + a_{I_t}^2)^{\frac{q}{2}}]}{\mathbb{E}[a_{I_1}^q]}. \quad (29)$$

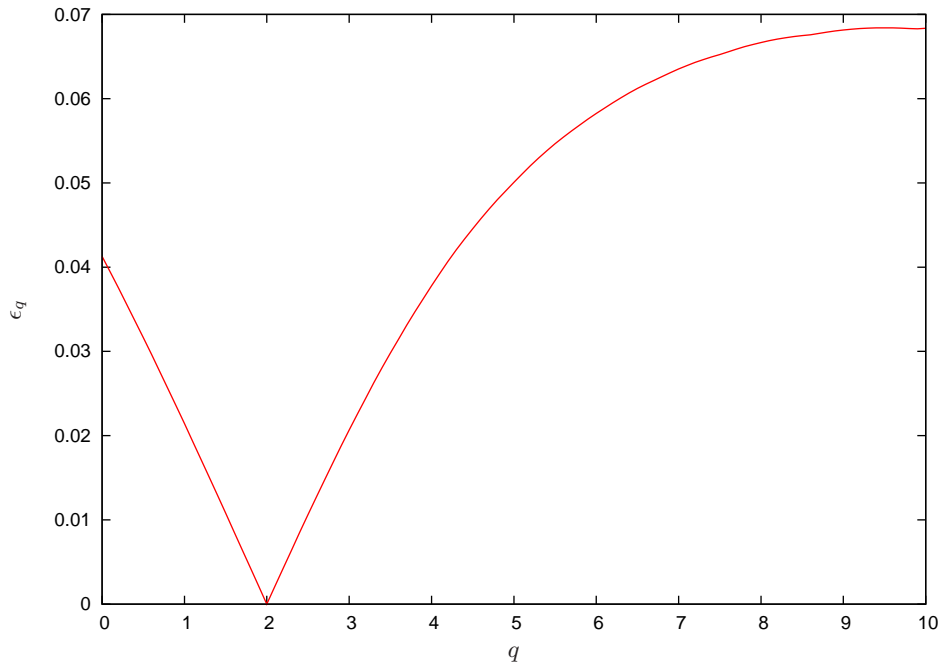


FIG. 1: Relative deviation of m_q^X from t^{qH_q} vs. q .

Notice in passing that the r.h.s. of Eq. (29) is well defined for any real q , even if $\mathbb{E}[|X_1|^q]$ diverges.

As we reported in the Main Text, m_q^X is well approximated for not too small values of D by the power t^{qH_q} with a generalized Hurst-like exponent H_q independent of t , thus allowing the model to exhibit pretty well-defined scaling properties at relatively short time scales. To corroborate this assertion, here we report a study of m_q^X based on numerical simulations for $M = 30$, $0.1 \leq D \leq 1/2$, and $t \leq M + 1$. We evaluate the exponent H_q with the least square method as follow:

$$qH_q \equiv \underset{H \in \mathbb{R}}{\operatorname{argmin}} \left\{ \sqrt{\frac{1}{M} \sum_{t=2}^{M+1} \left[\frac{\ln m_q^X(t)}{\ln t} - qH \right]^2} \right\} = \frac{1}{M} \sum_{t=2}^{M+1} \frac{\ln m_q^X(t)}{\ln t}. \quad (30)$$

Then, we measure the distance of m_q^X from t^{qH_q} with the relative mean fluctuation

$$\epsilon_q \equiv \max \left\{ \frac{1}{qH_q} \sqrt{\frac{1}{M} \sum_{t=2}^{M+1} \left[\frac{\ln m_q^X(t)}{\ln t} - qH_q \right]^2} : \nu \in [0, 1] \text{ and } D \in [0.1, 1/2] \right\}. \quad (31)$$

Even if not explicitly indicated, it is clear that m_q^X and H_q depend on ν and D . Fig. 1 shows ϵ_q vs. q , for q in between 0 and 10. The fact that $\epsilon_2 = 0$ is not surprising since $m_2^X(t) = t$ as one can immediately verify recalling the stationarity of $\{I_t\}_{t=1}^\infty$. For $q \neq 2$, we find values of ϵ_q of few points per cent. This confirms that m_q^X is close to t^{qH_q} and motivates the analysis of the exponent H_q . In Fig. 2 we report an explicit comparison between m_q^X and t^{qH_q} for $q = 0.5, 1, 3, 4$, $\nu = 0.01$, and $D = 0.25$. The corresponding H_q vs. q plot is shown in Fig. 1 of the Main Text.

Before we proceed to further investigate H_q , a remark is in order about small values of D . When D goes to 0, a_i vanishes if $i > 1$, thus approaching δ_{i1} . On the other hand, $\delta_{I_{11}}, \dots, \delta_{I_{t1}}$ are independent identically distributed Bernoulli variables, since in our model there is no correlations between restarts. Then, one can easily verify that in such a limit $m_q^X(t)$ takes the simple form

$$\sum_{n=1}^t n^{\frac{q}{2}} \binom{t}{n} \nu^{n-1} (1-\nu)^{t-n}. \quad (32)$$

This function is poorly approximated by a power of the time when q is small and ν assumes intermediate values: for instance, with $q = 0$ and $\nu = 1/2$, it reduces to $2(1 - 2^{-t})$. This is the reason that leads us to exclude small value of

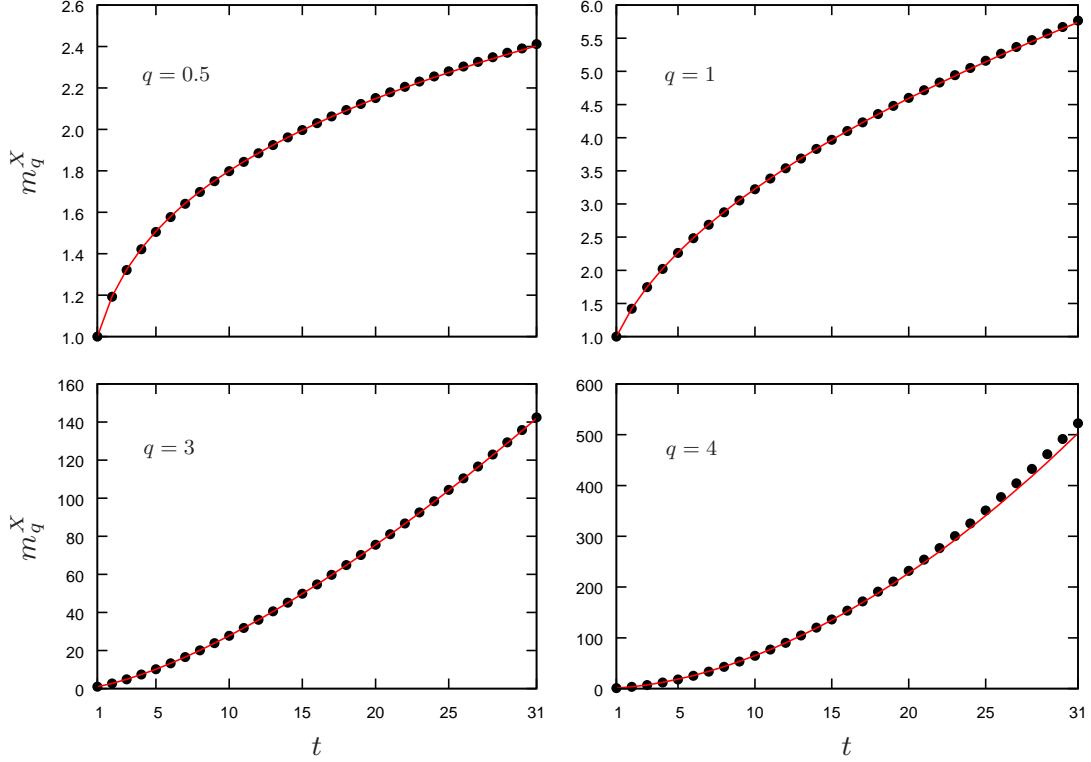


FIG. 2: Comparison between m_q^X (dots) and t^{qH_q} (dashed lines) for $t \leq 31$, $\nu = 0.01$, $D = 0.25$ and some values of q .

D and to focus on $D \geq 0.1$ in the scaling analysis. It is also worth noticing that ν is typically much smaller than $1/2$ in order to reproduce empirical financial data.

For the scaling exponent H_q defined by Eq. (30), we have $H_q \geq 1/2$ if $q \leq 2$ and $H_q \leq 1/2$ if $q > 2$. Indeed, the function

$$F(x_1, \dots, x_t) \equiv \left(x_1^{\frac{1}{\alpha}} + \dots + x_t^{\frac{1}{\alpha}} \right)^\alpha \quad (33)$$

is convex when $\alpha \leq 1$ and concave if $\alpha > 1$. Thus, setting $\alpha = q/2$, the Jensen's inequality and the stationarity of the process $\{I_t\}_{t=1}^\infty$ tell us that if $q \leq 2$ then

$$m_q^X(t) = \frac{\mathbb{E}[F(a_{I_1}^q, \dots, a_{I_t}^q)]}{\mathbb{E}[a_{I_1}^q]} \geq \frac{F(\mathbb{E}[a_{I_1}^q], \dots, \mathbb{E}[a_{I_t}^q])}{\mathbb{E}[a_{I_1}^q]} = t^{\frac{q}{2}}, \quad (34)$$

while for $q > 2$

$$m_q^X(t) = \frac{\mathbb{E}[F(a_{I_1}^q, \dots, a_{I_t}^q)]}{\mathbb{E}[a_{I_1}^q]} \leq \frac{F(\mathbb{E}[a_{I_1}^q], \dots, \mathbb{E}[a_{I_t}^q])}{\mathbb{E}[a_{I_1}^q]} = t^{\frac{q}{2}}. \quad (35)$$

The bounds on H_q then follow by its definition, Eq. (30). Fig. 3 shows the level curves of qH_q vs. ν and D in the range $[0, 1]$ and $[0.1, 1/2]$, respectively, and for different values of q . The exponent H_q displays large variations for small values of ν and D when $q > 2$ whereas it is close to $1/2$ in the other cases. Moreover, given ν we notice that H_q is a decreasing function of D if $q < 2$ and an increasing function if $q > 2$. Disentangling the contribution of ν and D to the scaling exponent is not easy. However, from the contour lines in Fig. 3 it is possible to appreciate how the variations of one of the two parameters can be compensated by modifications of the other.

We conclude the present analysis by studying analytically the limit of m_q^X when $D \leq 1/2$ and ν approaches zero. We shall make use of the symbol \sim of asymptotic equivalence introduced in the previous Section and the results in Eq. (25). The computation starts by isolating the trajectories corresponding to at most one restart from the others

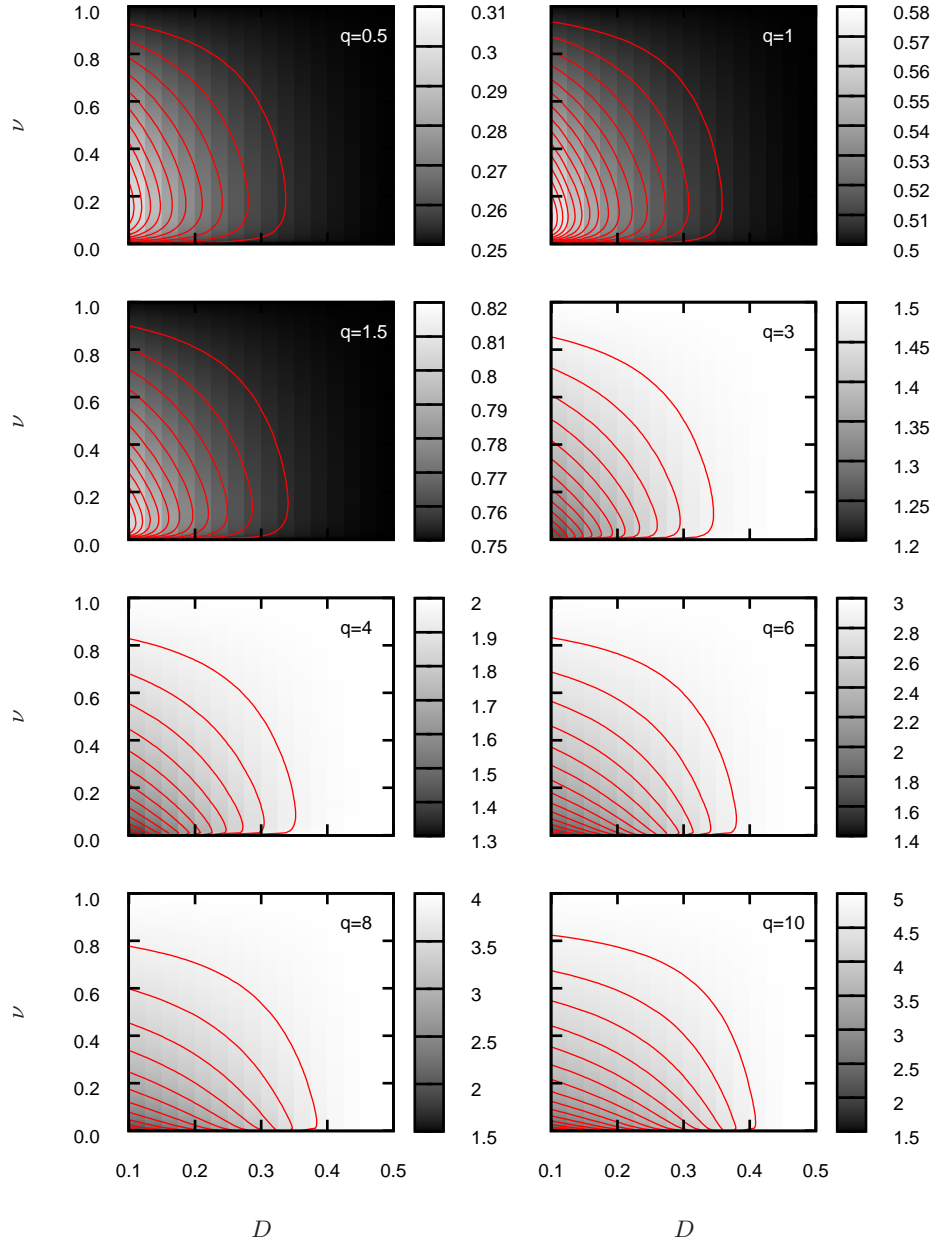


FIG. 3: Scaling exponent qH_q as a function of ν and D for several q . Contour lines are also shown.

in the numerator of m_q^X . Then, remembering $a_i^2 = i^{2D} - (i-1)^{2D}$ and assuming $t \geq 2$, we get the first equivalence

$$\begin{aligned} \mathbb{E}[(a_{I_1}^2 + \dots + a_{I_t}^2)^{\frac{q}{2}}] &\sim \sum_{i=1}^{\infty} [(i+t-1)^{2D} - (i-1)^{2D}]^{\frac{q}{2}} \nu(1-\nu)^{i+t-2} \\ &+ \sum_{\tau=2}^t \sum_{i=1}^{\infty} [(i+\tau-1)^{2D} - (i-1)^{2D} + (t-\tau+1)^{2D}]^{\frac{q}{2}} \nu^2(1-\nu)^{i+t-3}. \end{aligned} \quad (36)$$

Noticing now that

$$\lim_{i \rightarrow \infty} [(i+\tau-1)^{2D} - (i-1)^{2D} + (t-\tau+1)^{2D}]^{\frac{q}{2}} = (t-\tau+1)^{Dq} \quad (37)$$

and that $(t - \tau + 1)^{Dq}$ does not vanish for $\tau = 2, \dots, t$, we see that the second term in Eq. (36) is $\sim \nu \sum_{\tau=1}^{t-1} \tau^{Dq}$. Thus, Eq. (36) can be recast as

$$\mathbb{E}[(a_{I_1}^2 + \dots + a_{I_t}^2)^{\frac{q}{2}}] \sim \sum_{i=1}^{\infty} [(i+t)^{2D} - i^{2D}]^{\frac{q}{2}} \nu(1-\nu)^{i+t-1} + \nu \sum_{\tau=1}^t \tau^{Dq}, \quad (38)$$

which is valid also for $t = 1$. To obtain this relation we shifted the index i in the first sum of Eq. (36) and then we moved the first addend to the second term. Finally, since $\lim_{i \rightarrow \infty} i^{(1/2-D)q} [(i+t)^{2D} - i^{2D}]^{\frac{q}{2}} = (2Dt)^{\frac{q}{2}}$, Eq. (25) allows us to obtain

$$m_q^X(t) \sim \begin{cases} t^{\frac{q}{2}} & \text{if } (1/2 - D)q \leq 1; \\ \frac{\sum_{i=1}^{\infty} [(i+t)^{2D} - i^{2D}]^{\frac{q}{2}} + \sum_{\tau=1}^t \tau^{Dq}}{\sum_{i=1}^{\infty} [(i+1)^{2D} - i^{2D}]^{\frac{q}{2}} + 1} & \text{if } (1/2 - D)q > 1. \end{cases} \quad (39)$$

This asymptotic equivalence proves that $H_q = 1/2$ for $q \leq 2/(1-2D)$ at small values of ν , as anticipated in the Main Text. In order to intuitively understand the content of such a result, we notice that when the restart probability ν goes to zero the random time $\{I_t\}_{t=1}^{\infty}$ tends to flow without stopping but its starting value becomes affected by very large fluctuations due to its stationarity. At small values of q , the sequence $\{a_i^q\}_{i=1}^{\infty}$ does not decay fast enough to keep under control such fluctuations and only its tail plays a role, providing a normal scaling exponent.

VII. THE “NULL” AND THE “COMPLETE” MODEL

In the Main Text we considered two particular choices for the function ρ : one corresponded to fix σ to a particular value and, being the simplest possible choice, we referred to the “null model” in that case; and the other, given by Eq. (20) of the Main Text, was obtained distributing σ^2 according to an inverse-gamma distribution. The model associated to the latter choice for ρ was named the complete model. Here we give some details about the null model and prove that the endogenous component of the complete model is an ARCH process, as stated in the Main Text.

A. The null model

When σ is fixed to a particular value σ_0 , the PDF φ_t of Eq. (5) factors and, consequently, from Eq. (6) we have that the joint PDF f_t^Y also factors as

$$f_t^Y(y_1, \dots, y_t) = \prod_{n=1}^t \mathcal{N}_{\sigma_0}(y_n). \quad (40)$$

Within this setting, the endogenous component $\{Y_t\}_{t=1}^{\infty}$ then reduces to a sequence of independent normal variables, which is the simplest possible endogenous process that our model can produce, and the observed compound process becomes a random time change of the Brownian motion. Thus, we are recovering a discrete-time model with random time and constant average volatility. Indeed, without demanding mathematical rigor, if $(W_t)_{t \geq 0}$ is a standard Brownian motion independent of $\{I_t\}_{t=1}^{\infty}$, then $X_1 + \dots + X_t$ is distributed as $W_{\sigma_0^2[a_{I_1}^2 + \dots + a_{I_t}^2]}$ for any t when $\{Y_t\}_{t=1}^{\infty}$ is a sequence of i.i.d. normal variables with mean zero and variance σ_0^2 .

As we discussed in the Main Text and in Section V, if $D < 1/2$ we can have effective fat tails with tail index $2/(1-2D)$ in the distribution of X_1 by considering a small enough value of the restart probability ν . This is the only possibility to obtain such tails within the present instance of the model. The rescaling of ρ we considered in Section V simply consists in taking $\sigma_0 = \bar{\sigma}/\sqrt{\mathbb{E}[a_{I_1}^2]}$ here, with $\bar{\sigma}$ a parameter independent of ν .

B. The complete model

The peculiar ρ given in the Main Text by Eq. (20) allows us to explicitly integrate over σ in the expression of φ_t , which reduces to a multivariate Student distribution:

$$\varphi_t(y_1, y_2, \dots, y_t) = \frac{\Gamma(\frac{\alpha+t}{2})}{(\sqrt{\pi}\beta)^t \Gamma(\frac{\alpha}{2})} \left[1 + \frac{y_1^2 + y_2^2 + \dots + y_t^2}{\beta^2} \right]^{-\frac{\alpha+t}{2}}. \quad (41)$$

Within this setting, reformulating the endogenous component $\{Y_t\}_{t=1}^\infty$ in terms of stochastic variables, rather than only stating its PDF's, is interesting and useful. We write such process as

$$Y_t = \begin{cases} \beta \cdot Z_1 & \text{if } t = 1; \\ \sqrt{\beta^2 + Y_{\max\{1, t-M\}}^2 + \dots + Y_{t-1}^2} \cdot Z_t & \text{if } t > 1, \end{cases} \quad (42)$$

with a residual sequence $\{Z_t\}_{t=1}^\infty$ obviously defined as

$$Z_t = \begin{cases} Y_1/\beta & \text{if } t = 1; \\ Y_t/\sqrt{\beta^2 + Y_{\max\{1, t-M\}}^2 + \dots + Y_{t-1}^2} & \text{if } t > 1. \end{cases} \quad (43)$$

Here we show that $\{Z_t\}_{t=1}^\infty$ is a sequence of Student's t-distributed independent variables when φ_t is given by Eq. (41). According to the definition of the ARCH process [3], this fact makes $\{Y_t\}_{t=1}^\infty$ a pure ARCH process with Student's t-distributed return residuals, as anticipated in the Main Text. To be more precise, we can prove that

$$f_t^Z(z_1, \dots, z_t) = \prod_{n=1}^t \frac{\Gamma(\frac{\alpha_n+1}{2})}{\sqrt{\pi}\Gamma(\frac{\alpha_n}{2})} (1 + z_n^2)^{-\frac{\alpha_n+1}{2}}, \quad (44)$$

with $\alpha_n \equiv \alpha + \min\{n-1, M\}$. Notice that Z_t 's are identically distributed for $t \geq M+1$, but the stationarity of $\{Y_t\}_{t=1}^\infty$ and the boundary effects at $t=1$ prevent them to be identically distributed for any t . It is also worth mentioning that simulating the process $\{Y_t\}_{t=1}^\infty$ becomes rather simple thanks to the algorithm reported in Ref. [2], which adapts the Box-Muller transform for normally distributed variables to Student's t-distributed variables.

In order to prove Eq. (44) we study the expectation value $\mathbb{E}[F(Z_1, Z_2, \dots, Z_t)]$, being F a test function on \mathbb{R}^t . By definition, Eq. (43), we have

$$\begin{aligned} \mathbb{E}[F(Z_1, Z_2, \dots, Z_t)] &= \mathbb{E}\left[F\left(Y_1/\beta, Y_2/\sqrt{\beta^2 + Y_1^2}, \dots, Y_t/\sqrt{\beta^2 + Y_{\max\{1, t-M\}}^2 + \dots + Y_{t-1}^2}\right)\right] \\ &= \int_{\mathbb{R}} dy_1 \int_{\mathbb{R}} dy_2 \dots \int_{\mathbb{R}} dy_t F\left(y_1/\beta, y_2/\sqrt{\beta^2 + y_1^2}, \dots, y_t/\sqrt{\beta^2 + y_{\max\{1, t-M\}}^2 + \dots + y_{t-1}^2}\right) \cdot \\ &\quad \cdot f_t^Y(y_1, y_2, \dots, y_t). \end{aligned} \quad (45)$$

We then perform a change of variables from the old y_n 's into the new

$$z_n = \begin{cases} y_1/\beta & \text{if } n = 1; \\ y_n/\sqrt{\beta^2 + y_{\max\{1, n-M\}}^2 + \dots + y_{n-1}^2} & \text{if } 1 < n \leq t. \end{cases} \quad (46)$$

This relation can be inverted to express the y_n 's as a function of the z_n 's. Since clearly y_n only depends on z_1, z_2, \dots, z_n , the Jacobian matrix of the transformation is triangular and thus its determinant is easily found as

$$\beta \prod_{n=2}^t \sqrt{\beta^2 + y_{\max\{1, n-M\}}^2 + \dots + y_{n-1}^2}. \quad (47)$$

Here and below the y_n 's must be thought as functions of the z_n 's. Such a change of variables leads us to the identity

$$\begin{aligned} \mathbb{E}[F(Z_1, Z_2, \dots, Z_t)] &= \int_{\mathbb{R}} dz_1 \int_{\mathbb{R}} dz_2 \dots \int_{\mathbb{R}} dz_t F(z_1, z_2, \dots, z_t) \cdot \\ &\quad \cdot \beta \prod_{n=2}^t \sqrt{\beta^2 + y_{\max\{1, n-M\}}^2 + \dots + y_{n-1}^2} f_t^Y(y_1, y_2, \dots, y_t). \end{aligned} \quad (48)$$

Now, although lengthy, using Eqs. (6) and (41) at first and Eq. (46) at last, it is straightforward to see that

$$\begin{aligned}
& \beta \prod_{n=2}^t \sqrt{\beta^2 + y_{\max\{1, n-M\}}^2 + \cdots + y_{n-1}^2} f_t^Y(y_1, y_2, \dots, y_t) \\
&= \frac{\Gamma(\frac{\alpha+1}{2})}{\sqrt{\pi}\Gamma(\frac{\alpha}{2})} \left[1 + \frac{y_1^2}{\beta^2}\right]^{-\frac{\alpha+1}{2}} \prod_{n=2}^t \frac{\Gamma(\frac{\alpha_n+1}{2})}{\sqrt{\pi}\Gamma(\frac{\alpha_n}{2})} \left[1 + \frac{y_n^2}{\beta^2 + y_{\max\{1, n-M\}}^2 + \cdots + y_{n-1}^2}\right]^{-\frac{\alpha_n+1}{2}} \\
&= \prod_{n=1}^t \frac{\Gamma(\frac{\alpha_n+1}{2})}{\sqrt{\pi}\Gamma(\frac{\alpha_n}{2})} (1 + z_n^2)^{-\frac{\alpha_n+1}{2}}, \tag{49}
\end{aligned}$$

where $\alpha_n \equiv \alpha + \min\{n-1, M\}$. Hence

$$\mathbb{E}[F(Z_1, Z_2, \dots, Z_t)] = \int_{\mathbb{R}} dz_1 \int_{\mathbb{R}} dz_2 \cdots \int_{\mathbb{R}} dz_t F(z_1, z_2, \dots, z_t) \prod_{n=1}^t \frac{\Gamma(\frac{\alpha_n+1}{2})}{\sqrt{\pi}\Gamma(\frac{\alpha_n}{2})} (1 + z_n^2)^{-\frac{\alpha_n+1}{2}} \tag{50}$$

and this eventually confirms that the process $\{Z_t\}_{t=1}^{\infty}$ is distributed according to Eq. (44). \square

VIII. AUTOCORRELATION STRUCTURE

Here we discuss in some detail the autocorrelation r_q^X of the process $\{|X_t|^q\}_{t=1}^{\infty}$ introduced in the Main Text. To begin with, we notice that the independence between $\{Y_t\}_{t=1}^{\infty}$ and $\{I_t\}_{t=1}^{\infty}$ allows us to write

$$r_q^X(t) \equiv \frac{\mathbb{E}[|X_1|^q |X_t|^q] - \mathbb{E}[|X_1|^q]^2}{\mathbb{E}[|X_1|^{2q}] - \mathbb{E}[|X_1|^q]^2} = \frac{\mathbb{E}[a_{I_1}^q a_{I_t}^q] \mathbb{E}[|Y_1|^q |Y_t|^q] - \mathbb{E}[a_{I_1}^q]^2 \mathbb{E}[|Y_1|^q]^2}{\mathbb{E}[a_{I_1}^{2q}] \mathbb{E}[|Y_1|^{2q}] - \mathbb{E}[a_{I_1}^q]^2 \mathbb{E}[|Y_1|^q]^2}. \tag{51}$$

Although expectations involving $\{a_{I_t}\}_{t=1}^{\infty}$ are finite for any q , we restrict on values of q such that $\int_0^{\infty} \sigma^{2q} \rho(\sigma) d\sigma < \infty$ in order to ensure that also those involving $\{Y_t\}_{t=1}^{\infty}$ are finite. The analysis of r_q^X we propose is based on the preliminary study of the autocorrelations $r_q^{a_I}$ and r_q^Y of the processes $\{a_{I_t}^q\}_{t=1}^{\infty}$ and $\{|Y_t|^q\}_{t=1}^{\infty}$, respectively, which is the subject of the next two paragraphs. Eventually, we bring together the results to go back over r_q^X . We deal first with $r_q^{a_I}$.

A. The autocorrelation $r_q^{a_I}$

The autocorrelation $r_q^{a_I}$ can be conveniently manipulated once one knows the probability of $I_t = j$, given that $I_1 = i$. When $j < t$ the event $I_t = j$ occurs only as a consequence of a restart at the time $t - j + 1$ and no restarts during the following $j - 1$ steps, regardless of the value of I_1 . Thus, $\mathbb{P}[I_t = j | I_1 = i] = \nu(1 - \nu)^{j-1}$ if $j < t$. On the contrary, when $j \geq t$, the event $I_t = j$ is only possible if no restart occurs during the whole temporal interval up to time t , since a restart in between 1 and t would provide a value of I_t smaller than t . In such circumstances $I_t = I_1 + t - 1$ and then $\mathbb{P}[I_t = j | I_1 = i] = (1 - \nu)^{t-1} \delta_{j, i+t-1}$ if $j \geq t$. Thus,

$$\begin{aligned}
\mathbb{P}[I_t = j | I_1 = i] &= \begin{cases} \nu(1 - \nu)^{j-1} & \text{if } j < t; \\ (1 - \nu)^{t-1} \delta_{j, i+t-1} & \text{if } j \geq t \end{cases} \\
&= \mathbb{P}[I_1 = j] + \begin{cases} 0 & \text{if } j < t; \\ (1 - \nu)^{t-1} \delta_{j, i+t-1} - \nu(1 - \nu)^{j-1} & \text{if } j \geq t. \end{cases} \tag{52}
\end{aligned}$$

Coming back to $r_q^{a_I}$ and fixing $t \geq 2$, we notice that

$$\begin{aligned}
\mathbb{E}[a_{I_1}^q a_{I_t}^q] - \mathbb{E}[a_{I_1}^q]^2 &= \sum_{i=1}^{\infty} \sum_{j=1}^{\infty} a_i^q a_j^q \left(\mathbb{P}[I_t = j, I_1 = i] - \mathbb{P}[I_1 = j] \cdot \mathbb{P}[I_1 = i] \right) \\
&= \sum_{i=1}^{\infty} \sum_{j=1}^{\infty} a_i^q a_j^q \left(\mathbb{P}[I_t = j | I_1 = i] - \mathbb{P}[I_1 = j] \right) \mathbb{P}[I_1 = i] \\
&= \sum_{i=1}^{\infty} \sum_{j=t}^{\infty} a_i^q a_j^q \left((1 - \nu)^{t-1} \delta_{j, i+t-1} - \nu(1 - \nu)^{j-1} \right) \mathbb{P}[I_1 = i], \tag{53}
\end{aligned}$$

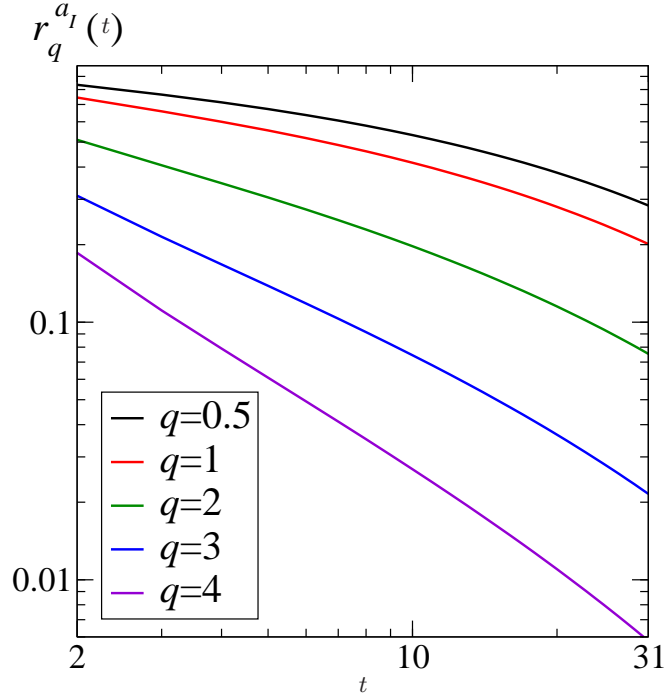


FIG. 4: Log-log plot of the short time autocorrelation of $\{a^q(I_t)\}_{i=1}^{\infty}$ for $\nu = 0.01$ and $D = 0.25$.

where the result stated in Eq. (52) has been used to get the last equality. Then,

$$\begin{aligned}
\mathbb{E}[a_{I_1}^q a_{I_t}^q] - \mathbb{E}[a_{I_1}^q]^2 &= (1-\nu)^{t-1} \sum_{i=1}^{\infty} a_i^q a_{i+t-1}^q \mathbb{P}[I_1 = i] - \mathbb{E}[a_{I_1}^q] \sum_{j=t}^{\infty} a_j^q \nu (1-\nu)^{j-1} \\
&= (1-\nu)^{t-1} \mathbb{E}[a_{I_1}^q a_{I_1+t-1}^q] - \mathbb{E}[a_{I_1}^q] \sum_{i=1}^{\infty} a_{i+t-1}^q \nu (1-\nu)^{i+t-2} \\
&= (1-\nu)^{t-1} \left(\mathbb{E}[a_{I_1}^q a_{I_1+t-1}^q] - \mathbb{E}[a_{I_1}^q] \mathbb{E}[a_{I_1+t-1}^q] \right), \tag{54}
\end{aligned}$$

the second equality being obtained through the substitution $j = i + t - 1$ in the second series. In summary, for the autocorrelation $r_q^{a_I}$ we find the more manageable expression:

$$\begin{aligned}
r_q^{a_I}(t) &= \frac{\mathbb{E}[a_{I_1}^q a_{I_t}^q] - \mathbb{E}[a_{I_1}^q]^2}{\mathbb{E}[a_{I_1}^{2q}] - \mathbb{E}[a_{I_1}^q]^2} \\
&= (1-\nu)^{t-1} \frac{\mathbb{E}[a_{I_1}^q a_{I_1+t-1}^q] - \mathbb{E}[a_{I_1}^q] \mathbb{E}[a_{I_1+t-1}^q]}{\mathbb{E}[a_{I_1}^{2q}] - \mathbb{E}[a_{I_1}^q]^2}, \tag{55}
\end{aligned}$$

which is valid also for $t = 1$ and allows us to investigate the correlation decay.

We point out that $r_q^{a_I}$ decays approximately according to a power law as t increases at short time scales if $D < 1/2$, whereas in the long time limit an exponential relaxation with rate $-\ln(1-\nu)$ dominates:

$$\lim_{t \rightarrow \infty} \frac{1}{t} \ln r_q^{a_I}(t) = \ln(1-\nu). \tag{56}$$

The former becomes the main trend at short time scales and small ν . For instance, Fig. 4 reports $r_q^{a_I}$ vs. t for $2 \leq t \leq 31$, $\nu = 0.01$ and $D = 0.25$ and for four different values of q . Moreover, for $q \leq 1/(1-2D)$, the smaller is ν , the more the correlations get persistent, as we already mentioned. We can understand this fact by looking at the limit behavior of $r_q^{a_I}$ when ν approaches zero. Making use of the symbol of asymptotic equivalence introduced in

Section V, we find

$$r_q^{a_I}(t) \sim \begin{cases} 1 & \text{if } (1 - 2D)q \leq 1; \\ \frac{\sum_{i=1}^{\infty} a_i^q a_{i+t-1}^q}{\sum_{i=1}^{\infty} a_i^{2q}} & \text{if } (1 - 2D)q > 1. \end{cases} \quad (57)$$

This result is an immediate consequence of Eqs. (55) and (25). As for the limit scaling behavior, the large fluctuations of I_1 affect $a_{I_1}^q$ when q is small enough. In addition, they also propagate to $a_{I_1+t-1}^q$ keeping intact the correlations.

B. The autocorrelation r_q^Y

The autocorrelation r_q^Y of the process $\{|Y_t|^q\}_{t=1}^{\infty}$ is much more difficult to investigate than the previous and in general we must resort to numerical simulations. Nevertheless it has a trivial structure for $t \leq M + 1$. Indeed, due to the exchangeability of $f_t^Y = \varphi_t$ if $t \leq M + 1$, we have that $\mathbb{E}[|Y_1|^q | Y_t|^q] = \mathbb{E}[|Y_1|^q | Y_2|^q]$ when $2 \leq t \leq M + 1$ and thus r_q^Y is independent of the time in such a temporal interval:

$$r_q^Y(t) = \frac{\mathbb{E}[|Y_1|^q | Y_2|^q] - \mathbb{E}[|Y_1|^q]^2}{\mathbb{E}[|Y_1|^{2q}] - \mathbb{E}[|Y_1|^q]^2}. \quad (58)$$

To the purpose of analyzing $r_q^Y(t)$ also for $t > M + 1$, we refer here to a favorable instance, corresponding to the function ρ given by Eq. (20) of the Main Text with $\alpha > 4$ and $q = 2$. As we know, such a ρ makes $\{Y_t\}_{t=1}^{\infty}$ an ARCH process for which the condition $\alpha > 4$ guarantees the existence of $\mathbb{E}[|Y_1|^4]$. We can then take advantage of the fact that, for ARCH processes, the expectation $\mathbb{E}[F(Y_1)Y_t^2]$ can be recursively computed for any t and any test function F for which it makes sense. Indeed, recalling Eq. (42), for $t \geq 2$ we can write

$$Y_t^2 = \left(\beta^2 + \sum_{n=1}^{\min\{t-1, M\}} Y_{t-n}^2 \right) Z_t^2. \quad (59)$$

Thus, noticing that Y_n is independent of Z_t if $n < t$ and bearing in mind that $Y_1 = \beta Z_1$, we have the simple chain of equalities

$$\begin{aligned} \mathbb{E}[F(Y_1)Y_t^2] - \mathbb{E}[F(Y_1)] \cdot \mathbb{E}[Y_1^2] &= \mathbb{E}\left[F(Y_1) \left(\beta^2 + \sum_{n=1}^{\min\{t-1, M\}} Y_{t-n}^2 \right) Z_t^2\right] - \mathbb{E}[F(Y_1)] \cdot \mathbb{E}[Y_1^2] \\ &= \mathbb{E}\left[F(Y_1) \left(\beta^2 + \sum_{n=1}^{\min\{t-1, M\}} Y_{t-n}^2 \right)\right] \cdot \mathbb{E}[Z_t^2] - \mathbb{E}[F(Y_1)] \cdot \mathbb{E}[Y_1^2] \\ &= \mathbb{E}[F(Y_1)] \left(\beta^2 \mathbb{E}[Z_t^2] - \mathbb{E}[Y_1^2] \right) + \mathbb{E}[Z_t^2] \cdot \sum_{n=1}^{\min\{t-1, M\}} \mathbb{E}[F(Y_1)Y_{t-n}^2] \\ &= \mathbb{E}[F(Y_1)] \left(\beta^2 \mathbb{E}[Z_t^2] - \mathbb{E}[Y_1^2] + \min\{t-1, M\} \mathbb{E}[Z_t^2] \mathbb{E}[Y_1^2] \right) + \\ &+ \mathbb{E}[Z_t^2] \cdot \sum_{n=1}^{\min\{t-1, M\}} \left(\mathbb{E}[F(Y_1)Y_{t-n}^2] - \mathbb{E}[F(Y_1)] \cdot \mathbb{E}[Y_1^2] \right) \\ &= \beta^2 \mathbb{E}[F(Y_1)] \left(\mathbb{E}[Z_t^2] - \mathbb{E}[Z_1^2] + \min\{t-1, M\} \mathbb{E}[Z_t^2] \mathbb{E}[Z_1^2] \right) + \\ &+ \mathbb{E}[Z_t^2] \cdot \sum_{n=1}^{\min\{t-1, M\}} \left(\mathbb{E}[F(Y_1)Y_{t-n}^2] - \mathbb{E}[F(Y_1)] \cdot \mathbb{E}[Y_1^2] \right). \end{aligned} \quad (60)$$

On the other hand, for the variables Z_t 's distributed according to Eq. (44) we have

$$\mathbb{E}[|Z_t|^q] = \frac{\Gamma\left(\frac{q+1}{2}\right)\Gamma\left(\frac{\alpha_t-q}{2}\right)}{\sqrt{\pi}\Gamma\left(\frac{\alpha_t}{2}\right)}, \quad (61)$$

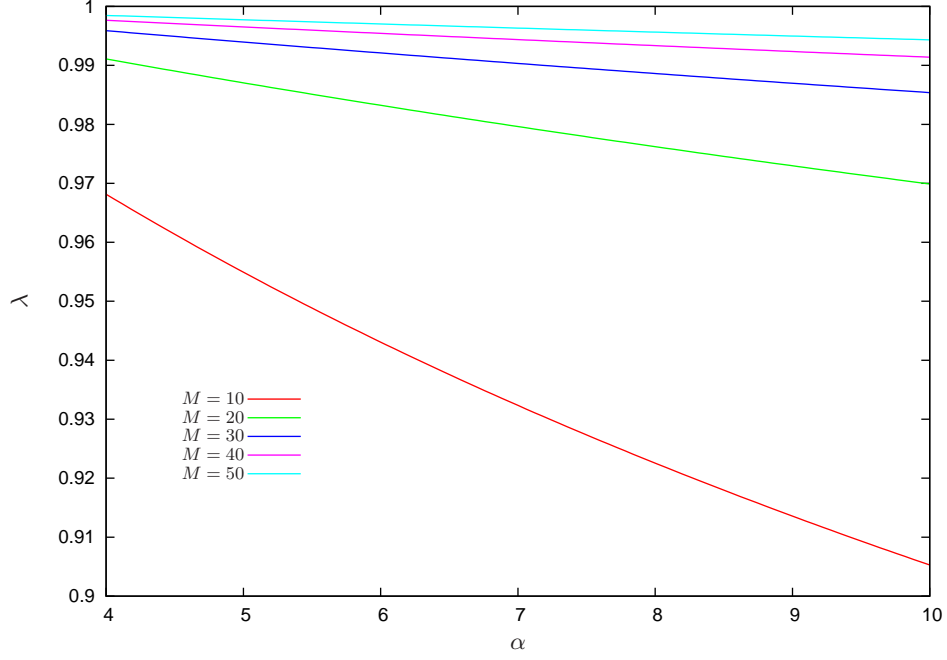


FIG. 5: Rate λ as a function of α for different values of M .

with $\alpha_t = \alpha + \min\{t - 1, M\}$. Thus, to verify that

$$\mathbb{E}[Z_t^2] - \mathbb{E}[Z_1^2] + \min\{t - 1, M\}\mathbb{E}[Z_t^2]\mathbb{E}[Z_1^2] = 0 \quad (62)$$

is not difficult once one sets $q = 2$ in Eq. (61). Combining Eq. (60) with Eq. (62), we eventually obtain the result

$$\mathbb{E}[F(Y_1)Y_t^2] - \mathbb{E}[F(Y_1)] \cdot \mathbb{E}[Y_1^2] = \frac{1}{\alpha_t - 2} \sum_{n=1}^{\min\{t-1, M\}} \left(\mathbb{E}[F(Y_1)Y_{t-n}^2] - \mathbb{E}[F(Y_1)] \cdot \mathbb{E}[Y_1^2] \right), \quad (63)$$

which establishes a recursive scheme to compute $\mathbb{E}[F(Y_1)Y_t^2] - \mathbb{E}[F(Y_1)] \cdot \mathbb{E}[Y_1^2]$.

Assuming $\alpha > 4$, setting $F(y) = y^2$ in Eq. (63), and dividing by $\mathbb{E}[|Y_1|^4] - \mathbb{E}[|Y_1|^2]^2$, we get a simple tool to evaluate $r_2^Y(t)$ for any t and to study its asymptotic behavior. In particular, as expected we find that if $2 \leq t \leq M + 1$ $r_2^Y(t)$ is independent of the time and equal to $1/(\alpha - 1)$, while for $t > M + 1$

$$r_2^Y(t) = \frac{1}{\alpha + M - 2} \cdot \sum_{n=1}^M r_2^Y(t - n). \quad (64)$$

In order to elucidate the asymptotic decay of r_2^Y , it is interesting to consider the function

$$F(x) \equiv \frac{1}{\alpha + M - 2} \cdot \sum_{n=1}^M \frac{1}{x^n} \quad (65)$$

for positive x . This is a strictly decreasing positive continuous function which diverges to infinity when $x \rightarrow 0^+$ and goes to zero when $x \rightarrow +\infty$. Thus, there exists a unique positive λ such that $F(\lambda) = 1$, which is smaller than 1 since $F(1) = M/(M + \alpha - 2) < 1$. The interest of this is that from Eq. (64) we have that r_2^Y decays exponentially fast with rate $-\ln \lambda$. Fig. 5 shows λ vs. α for different values of the memory M . Not surprisingly, the correlations have a slower decay at higher values of M . Also, the decay rate is minimum when α goes towards the lower limit value of 4, namely when the distribution of Y_1 displays the most pronounced tails. To show that λ really rules the decay of r_2^Y , we prove by induction that

$$\frac{\lambda^{t-2}}{\alpha - 1} \leq r_2^Y(t) \leq \frac{\lambda^{t-M-1}}{\alpha - 1} \quad (66)$$

if $t \geq 2$. These bounds then entail that

$$\lim_{t \rightarrow \infty} \frac{1}{t} \ln r_2^Y(t) = \ln \lambda . \quad (67)$$

We focus on the second inequality only, as the first can be treated with the same arguments. Since $\lambda < 1$ we have that $\lambda^{t-M-1}/(\alpha-1) \geq 1/(\alpha-1) = r_2^Y(t)$ for t in between 2 and $M+1$. Fixing then $t > M+1$ and assuming that the inequality holds up to $t-1$, we see that

$$r_2^Y(t) \leq \frac{1}{\alpha + M - 2} \cdot \sum_{n=1}^M \frac{\lambda^{t-n-M-1}}{\alpha - 1} = \frac{\lambda^{t-M-1}}{\alpha - 1} \cdot F(\lambda) = \frac{\lambda^{t-M-1}}{\alpha - 1} . \quad (68)$$

C. The autocorrelation r_q^X

We now bring together the above results to discuss the behavior of r_q^X . Eq. (51) tell us that

$$r_q^X(t) = u_q + v_q r_q^{a_I}(t). \quad (69)$$

If $2 \leq t \leq M+1$ the coefficients u_q and v_q are independent of time:

$$u_q \equiv \frac{\mathbb{E}[|Y_1|^q | Y_2|^q] - \mathbb{E}[|Y_1|^q]^2}{\mathbb{E}[a_{I_1}^{2q}] \mathbb{E}[|Y_1|^{2q}] - \mathbb{E}[a_{I_1}^q]^2 \mathbb{E}[|Y_1|^q]^2} \cdot \mathbb{E}[a_{I_1}^q]^2, \quad (70)$$

$$v_q \equiv \frac{\mathbb{E}[a_{I_1}^{2q}] - \mathbb{E}[a_{I_1}^q]^2}{\mathbb{E}[a_{I_1}^{2q}] \mathbb{E}[|Y_1|^{2q}] - \mathbb{E}[a_{I_1}^q]^2 \mathbb{E}[|Y_1|^q]^2} \cdot \mathbb{E}[|Y_1|^q | Y_2|^q]. \quad (71)$$

Thus, at short time scales the autocorrelation r_q^X entirely inherits the time dependence of $r_q^{a_I}$, as we mentioned in the Main Text. Notice that $u_q = 0$ when the endogenous $\{Y_t\}_{t=1}^\infty$ process reduces to a sequence of independent variables and in such a case Eq. (69) holds for any t . More in general, for any t we can rewrite Eq. (51) as

$$r_q^X(t) = u_q(t) r_q^Y(t) + v_q r_q^{a_I}(t) \quad (72)$$

where we have again used the letters u_q and v_q but with a different meaning. Here u_q is the positive function of the time

$$u_q(t) \equiv \frac{\mathbb{E}[|Y_1|^{2q}] - \mathbb{E}[|Y_1|^q]^2}{\mathbb{E}[a_{I_1}^{2q}] \mathbb{E}[|Y_1|^{2q}] - \mathbb{E}[a_{I_1}^q]^2 \mathbb{E}[|Y_1|^q]^2} \cdot \mathbb{E}[a_{I_1}^q a_{I_t}^q] \quad (73)$$

and v_q the positive coefficient

$$v_q \equiv \frac{\mathbb{E}[a_{I_1}^{2q}] - \mathbb{E}[a_{I_1}^q]^2}{\mathbb{E}[a_{I_1}^{2q}] \mathbb{E}[|Y_1|^{2q}] - \mathbb{E}[a_{I_1}^q]^2 \mathbb{E}[|Y_1|^q]^2} \cdot \mathbb{E}[|Y_1|^q]^2 . \quad (74)$$

Since

$$\lim_{t \rightarrow \infty} u_q(t) = \frac{\mathbb{E}[|Y_1|^{2q}] - \mathbb{E}[|Y_1|^q]^2}{\mathbb{E}[a_{I_1}^{2q}] \mathbb{E}[|Y_1|^{2q}] - \mathbb{E}[a_{I_1}^q]^2 \mathbb{E}[|Y_1|^q]^2} \cdot \mathbb{E}[a_{I_1}^q]^2 > 0 , \quad (75)$$

when ρ is given by Eq. (20) of the Main Text (for which we know the behavior of r_q^Y in the instance $q = 2$) we find that

$$\lim_{t \rightarrow \infty} \frac{1}{t} \ln r_2^X(t) = \ln \max\{\lambda, 1 - \nu\} . \quad (76)$$

Thus, within this setting the autocorrelation of the observed process decays exponentially fast in the long time limit. The slowest between the relaxation rates of r_2^Y and $r_2^{a_I}$ determine the one of r_q^X .

Acknowledgments

This work is supported by “Fondazione Cassa di Risparmio di Padova e Rovigo” within the 2008-2009 “Progetti di Eccellenza” program.

-
- [1] W. Feller, *An Introduction to Probability Theory and its Applications*, Vol. II (John Wiley & Sons, New York, 1971).
 - [2] R.W. Bailey, *Mathematics of Computation* **62**, 779 (1994).
 - [3] R.S. Tsay, *Analysis of Financial Time Series* (John Wiley & Sons, 2002).